Review article

Felix Sima, Koji Sugioka*, Rebeca Martínez Vázquez*, Roberto Osellame, Lóránd Kelemen* and Pal Ormos

Three-dimensional femtosecond laser processing for lab-on-a-chip applications

https://doi.org/10.1515/nanoph-2017-0097
Received September 30, 2017; revised November 27, 2017; accepted December 8, 2017

Abstract: The extremely high peak intensity associated with ultrashort pulse width of femtosecond laser allows us to induce nonlinear interaction such as multiphoton absorption and tunneling ionization with materials that are transparent to the laser wavelength. More importantly, focusing the femtosecond laser beam inside the transparent materials confines the nonlinear interaction only within the focal volume, enabling three-dimensional (3D) micro- and nanofabrication. This 3D capability offers three different schemes, which involve undeformative, subtractive, and additive processing. The undeformative processing preforms internal refractive index modification to construct optical microcomponents including optical waveguides. Subtractive processing can realize the direct fabrication of 3D microfluidics, micromechanics, microelectronics, and photonic microcomponents in glass. Additive processing represented by two-photon polymerization enables the fabrication of 3D polymer micro- and nanostructures for photonic and microfluidic devices. These different schemes can be integrated to realize more functional microdevices including lab-on-a-chip devices, which are miniaturized laboratories that can perform reaction, detection, analysis, separation, and synthesis of biochemical materials with high efficiency, high speed, high sensitivity, low reagent consumption, and low waste production. This review paper describes the principles and applications of femtosecond laser 3D micro- and nanofabrication for lab-on-a-chip applications. A hybrid technique that promises to enhance functionality of lab-on-a-chip devices is also introduced.

Keywords: femtosecond lasers; lab-on-a-chip; subtractive manufacturing; additive manufacturing; 3D fabrication.

***Corresponding authors: Koji Sugioka,** RIKEN Center for Advanced Photonics, 2-1 Hirosawa, Wako, Saitama 351-0198, Japan, e-mail: ksugioka@riken.jp; **Rebeca Martínez Vázquez,** Istituto di Fotonica e Nanotecnologie (IFN)-CNR and Dipartimento di Fisica-Politecnico di Milano, Piazza Leonardo da Vinci 32, 20133 Milan, Italy, e-mail: rebeca.martinez@polimi.it; and
Lóránd Kelemen, Biological Research Centre, Institute of Biophysics, Hungarian Academy of Sciences, Temesvári krt. 62, 6726 Szeged, Hungary, e-mail: kelemen.lorand@brc.mta.hu
Felix Sima: RIKEN Center for Advanced Photonics, 2-1 Hirosawa, Wako, Saitama 351-0198, Japan; and CETAL, National Institute for Lasers, Plasma and Radiation Physics, Magurele, Ilfov 00175, Romania
Roberto Osellame: Istituto di Fotonica e Nanotecnologie (IFN)-CNR and Dipartimento di Fisica-Politecnico di Milano, Piazza Leonardo da Vinci 32, 20133 Milan, Italy
Pal Ormos: Biological Research Centre, Institute of Biophysics, Hungarian Academy of Sciences, Temesvári krt. 62, 6726 Szeged, Hungary

1 Introduction

Lab-on-a-chip (LOC) is defined as miniaturized devices capable of integrating laboratory functions for advanced high throughput reactions and analyses with high sensitivity using low quantities of reagents and reduced costs [1, 2]. In the literature, they are a subset of MicroElectroMechanical Systems (MEMS) [3] and are sometimes equivalent to micro total analysis systems (μTAS) [4]. LOCs involve microfluidic, optofluidic, and electrofluidic devices [5–8]. Their applications found great interests in clinical diagnostics, environmental monitoring, chemical and biological warfare surveillance, and food industry [9]. Common biochemical testing platforms that allow assays with an array of a hundred different reagents with a microliter volume are thus replaced by the LOC assembling that can reduce the volume to nano- to picoliter levels. Such microfluidic structures with geometrically nonconventional configurations can evidence special physical and chemical properties such as pressure gradients, capillarity, and diffusivity that allow precise control and manipulation of small volumes of fluids [10, 11]. By decreasing the dimensions and volume sizes of the miniaturized devices, the number of molecules available for detection can be reduced [12, 13]. Further, such integrated on-chip

detection systems would realize a very high sensitivity measurement of very low analyte concentrations [13] or even single-cell detection and manipulation [14]. One can expect to use these useful integrated platforms for analytical biochemistry based on electrochemical and optical detection schemes [15–18]. Most common techniques for fabrication of these devices are photo-lithography and soft lithography by which polydimethylsiloxane (PDMS) is generally casted on negative tone photoresist masters to fabricate complex microfluidic configurations [11, 19, 20]. Several advantages of PDMS include biocompatibility, transparency, and ease of use, but it exhibits also some disadvantages such as nonreusability, requirement of multiple stacking processing, and adsorbant of organic compounds [21].

On the other hand, femtosecond lasers, defined as lasers emitting pulsed beams with durations from tens to hundreds of femtoseconds, are used nowadays for high-quality micro- and nanofabrication. Specifically, energy deposition at a time scale shorter than electron-phonon coupling processes in any materials due to the ultrashort pulse width can suppress the formation of heat-affected zone allowing laser processing with high precision and resolution [22]. The unique advantage of femtosecond laser processing over conventional methods resides in the capability of sculpturing complex three-dimensional (3D) shapes at micro- and nanoscales in transparent materials, both inorganic and organic. Indeed, by employing focused ultrashort pulses with extremely high peak intensities, one can precisely set the interaction region at a localized area of either surfaces or in volume [23–25]. This feature can not only completely eliminate complicated multiple stacking processing combined with patterning process based on photolithography for 3D fabrication but also create complex 3D structures that are not achievable by other conventional methods. As a consequence, femtosecond laser technologies are increasingly developed and then extensively applied to the fabrication of LOC devices made of either inorganic, organic, or composite transparent and biocompatible materials with high degree of precision and reproducibility [26]. Thus, versatile 3D microfluidic chips, in which multifunctional components as well as specific functions are integrated in a tiny chip, are now ready to be fabricated by the femtosecond laser technologies [27–29].

Another advantage of the femtosecond laser is that it can perform three different schemes in 3D processing, which are categorized as undeformative, subtractive and additive processing. A typical undeformative process appears when microscopic modifications are generated by femtosecond laser processing without macroscopic volume changes. It is generally applied to 3D optical waveguide (WG) or other micro-optical component writing inside the glass based on permanent refractive index change [30]. A concrete advantage of such structures appears when they are integrated in glass microfluidic structures which proves very beneficial for fabrication of highly functional biochips, although the microfluidic structures must be prepared in advance by other technique. This technique is thus utilized to integrate the optical WGs in the LOC devices to deliver light beams and collect optical signals for biochemical analysis by optical means.

One of the subtractive 3D processing methods is referred to as femtosecond laser-assisted etching (FLAE) or femtosecond laser irradiation followed by chemical etching, in which femtosecond laser direct writing and subsequent chemical wet etching are carried out to create 3D hollow microstructures inside glass [31–33]. FLAE is applied to flexibly fabricate complex, 3D microfluidic channels in glass [15, 34, 35]. Another subtracting processing for fabrication of 3D glass microfluidic structures is femtosecond laser direct ablation of glass in water (water-assisted femtosecond laser drilling, WAFLD) [36]. By such subtractive methods one can directly fabricate microfluidic circuits in glasses on large areas without processes of multiple stacking and bonding. One can further preserve specific characteristics of glass such as robustness, portability, and transparency, while eventual drawbacks reside in low fabrication resolution and low flexibility in terms of materials due to limited availability of a specific type of glass for this process.

The additive 3D processing is represented by two-photon polymerization (TPP). Unlike single-photon polymerization using UV light which occurs along the entire exposed pattern, TPP by irradiation of photo-curable resin or negative photoresists with femtosecond laser can take place only at the focal point to solidify polymer with nanometric resolution [37]. Three-dimensional complex nanostructures are then developed by translating the focal point within the resin [38, 39]. The main advantage of this technology is the precise localization of 3D structures that can be further sculptured with nanoscale feature sizes by translating the focal point of laser within the photosensitive resin. The capability of controlling the feature sizes in the micro- and nanoscale and high flexibility arising from laser direct writing scheme has pushed TPP to become a well-known technology for fabricating micro- and nanodevices with complex designs, including filters [40], fluid mixer [41], microlens [42], etc. in LOCs. An inherent drawback is related to the extension capability to large-scale processing.

Thus, each scheme of 3D processing has both advantages and disadvantages. In fact, one scheme of 3D processing can create not any kinds of structures and functions. A hybrid technique of different schemes can create much more complex 3D structures and thereby promises to enhance functionality of LOC devices. For example, a successive procedure of subtractive FLAE and the undeformative optical WG writing realized optofluidics for detection, manipulation, and sorting of bio samples [30, 43–45]. In addition, an innovative "ship-in-a-bottle" technology combining subtractive FLAE of glasses and additive TPP [46] is not only an instrument that can tailor 3D environments at submicrometric level but also a tool to fabricate biomimetic structures inside a closed glass microfluidic chip [47]. Specifically, FLAE can flexibly fabricate 3D microfluidic structures embedded in glass microchips without a complicated procedure of stacking and bonding of glass substrates. Successive TPP can directly integrate complex shapes of polymer structures with a submicrometer feature size due to its high fabrication resolution to create biomimetic structures inside the glass microfluidics [48, 49].

In this review, we will first concentrate to introduce each scheme of the undeformative, subtractive, and additive 3D femtosecond laser processing (3D-FLP) of transparent materials such as glasses and photoresists for the fabrication of functional LOCs. The glass is a suitable material as a biochip platform due to robustness, easy manipulation, and high portability, while optionally, polymeric structures could provide the submicron features and elasticity necessary for specific biomedical applications. Besides the microfluidic channels, due to the capability and flexibility of fabricating 3D geometries, functional microcomponents can be fabricated along or inside microfluidic devices for specific biological assays. To further demonstrate excellent capability of the 3D-FLP for the fabrication of LOCs, hybrid technique of different schemes is also introduced.

2 Principle of femtosecond laser 3D processing

The 1990s decade set the birth of femtosecond laser 3D processing, with the publication of the first results about femtosecond laser ablation of micro features in glass and silver [50, 51] immediately followed by the first femtosecond laser permanent modification in the bulk of transparent dielectric materials [52]. Since then there have been several studies about FLP of materials, but there is still missing a complete physical model that explains it [24, 26]. However, there are some certainties that we will briefly present and discuss along this section.

Three-dimensional processing by femtosecond laser radiation is a nonlinear process; the transparency of the material at the laser wavelength used (near infrared or visible) and the high peak intensity reached by the focused femtosecond laser must involve nonlinear absorption processes to obtain the permanent modification of the material. Moreover, due to this nonlinear nature, the modification will take place just near the focal region, and thus by translating the sample with respect to the laser beam, we will create arbitrary 3D modified regions embedded in the pristine sample. Exposure parameters including laser wavelength, pulse energy, pulse duration, repetition rate, polarization, focal length, and scan speed directly influence the characteristics of the final processing.

Due to the different nature of the physical phenomena and morphological effects on the material, we will separately study FLP for dielectrics and photosensitive resins.

2.1 Femtosecond laser processing of dielectrics

Dielectrics constitutes a broad material family with different physical and chemical characteristics, so the modification regime strongly depends on original properties such as bandgap, thermal conductivity, and working point temperature. Despite this heterogeneity, the modification process always follows three main steps: start with the generation of a free electron plasma, followed by an energy relaxation that finally conducts to the permanent modification of the material.

Femtosecond laser photons (with λ ranging from 500 nm to 1040 nm) do not have enough energy to promote electrons from valence band to conduction band; i.e. the photon energy is too low to overcome the energy bandgap (E_g) in transparent substrates. Therefore, electrons can be strongly promoted only by nonlinear processes that become statistically relevant with high incident photon flux, meaning that these phenomena are activated by high-intensity laser beams [52].

Laser pulses with duration of tens/hundreds of femtoseconds are indeed needed to reach high enough peak intensities (around 10^{13} W/cm^2). Two competing nonlinear absorption phenomena are responsible for plasma activation: multiphoton ionization and tunneling ionization. Multiphoton ionization occurs when multiple photons are absorbed by an electron in the valence band, leading

to a promotion to the conduction band. The number of photons N required to bridge the bandgap must satisfy the following:

$$NE_{ph} > E_g, \tag{1}$$

where E_{ph} is the energy of a single photon. In tunneling ionization, the strong electromagnetic field of femtosecond laser pulses distorts the band structure and reduces the potential barrier between valence and conduction bands. Therefore, direct band-to-band transitions may proceed by quantum tunneling of the electron through the bandgap. The transition between these two competing processes is described by the Keldysh parameter γ:

$$\gamma = \frac{\omega}{e}\sqrt{\frac{c\, n \epsilon_0 E_g\, m_e}{I}} \tag{2}$$

where ω is the laser angular frequency, e is the electron charge, m_e is the effective electron mass, c is the speed of light in vacuum, n is the linear refractive index of the substrate, ϵ_0 is the permittivity of free space, and I is the laser intensity at the focus [53]. If $\gamma \gg 1.5$, multiphoton ionization dominates; if $\gamma \ll 1.5$, tunneling is predominant; and if $\gamma \approx 1.5$, nonlinear absorption is a combination of tunneling and multiphoton ionizations.

A third phenomenon that contributes to the plasma activation is free carrier absorption, by which an electron in the conduction band might absorb several photons and reach an energy that exceeds the conduction band minimum by more than the bandgap energy. That hot electron will then impact, and ionize, a bound electron in the valence band resulting in two excited electrons at the conduction band minimum. This process can repeat itself as long as the laser field is present giving rise to an electron avalanche. Avalanche ionization requires a minimum number of "seed" electrons in the conduction band to take place; these electrons might be provided by defect states or thermally excited impurities or by direct multiphoton or tunneling ionization.

As a consequence, the density of electrons in the conduction band grows until the plasma frequency equals the laser frequency, where optical breakdown takes place and most of the incident laser energy is absorbed by the electron plasma [23]. This hot electron plasma relaxes transferring its energy to the lattice, but since the lattice heating time is around tens of picoseconds, the energy is transferred long after the laser pulse is gone. This decoupling between energy absorption and lattice heating, together with the fact that short pulses need less energy to achieve the intensity for optical breakdown, allows obtaining more precise machining with femtosecond lasers than with longer pulse lasers.

Because of this energy transfer into the lattice, a permanent morphological modification of the material takes place, and depending on irradiation conditions and material properties, it will have different characteristics. In general, we can classify them into three main structural changes [52, 54]: the material suffers a local change on its refractive index [52], generation of self-organized nanoscale layered structures resulting in a local birefringence [54, 55], and the generation of empty voids inside the material [56, 57].

2.2 Two photon polymerization

Femtosecond laser TPP is a nonlinear process in which 3D free-standing polymer structures are created by the laser-assisted photopolymerization of a photoresist. This technique is based on the exposure of a resin by a tightly focused femtosecond laser beam, enabling the polymerization of a small volume at the focal point. Moving the laser beam relative to the sample, it is possible to create arbitrary 3D sculptures with submicrometer resolution, after washing out the nonpolymerized photoresist.

TPP is based on the physical phenomenon of two-photon absorption (TPA), in which two photons are absorbed almost simultaneously (~10^{-5} s) by an atom or molecule, exciting it to a higher energy level [58]. This nonlinear absorption will initiate the polymerization reaction, in which development depends on the photoresist used. Let us introduce the processes involved in the polymerization of negative-tone photoresist, which are the most commonly used in TPP.

A first type of polymerization reaction is radicalic polymerization [37]. This mechanism is found, for example, in acrylate resists, and it consists in the generation of free radicals, with the help of a photoinitiator. Free radicals are molecules with an unpaired electron, usually electrically neutral, that are extremely reactive. A photoinitiator is a molecule that absorbs light through TPA with very high quantum efficiency. Upon energy absorption, the photoinitiator splits into the free radicals that start a chain polymerization reaction. The initial free radicals bond to monomers generating more radicals at their end. The reaction propagates bonding more monomers to the chain, growing in size, until it is terminated when two radicals meet.

Polymerization can also be started by cations generation. The chain mechanism is similar to the radicalic

one, but in this case a catalytic photoacid is created that starts the voxel formation. The bonds generated in this way are still not resistant to solvent washing; therefore, the material must undergo a post exposure treatment, which consists usually in baking the resist to complete the polymerization. In TPP, this step can be sometimes avoided, since the heat generated by laser irradiation can be sufficient to avoid bond breaking [59]. Common materials polymerized in this way are epoxides and vinyl ethers.

Although the technique is widely known as TPP, there can also be simultaneous absorption of more than two photons or other nonlinear phenomena concurring in starting the polymerization reaction, such as multiphoton ionization, depending on the irradiation regime [60]. Due to the nonlinear nature of multi-photon absorption and the existence of an intensity threshold for polymerization, the resolution attainable by TPP is finer than that expected by diffraction limit. In fact, resolutions of 100 nm have been demonstrated [39], and a further enhancement is possible in depletion-based configurations [61].

From a processing point of view, the different modifications just introduced permit us to divide the FLP into three main categories:

1. Undeformative processing, in which photonic devices are created in the bulk of the pristine sample just by changing the refractive index.
2. Subtractive processing, in which the irradiated material is removed from the original sample.
3. Additive processing, in which new structures are created on the original sample.

Moreover, the high flexibility of this technology allows to introduce a forth category in which these different regimes are mixed in what we call “hybrid processing”.

3 Undeformative processing

Femtosecond lasers are an extremely versatile tool for the fabrication of optical circuits due to its 3D nature and its high versatility in terms of processing material. These two characteristics have permitted the rapid diffusion of this tool in the field of integrated optics [44, 62] for the fabrication of passive and active 3D photonic devices such as optical couplers and splitters [63], Mach-Zehnder interferometers (MZI) [64], volume Bragg gratings [65], diffractive lenses [66], optical lanterns [67], or WG lasers [68, 69]. It is over the scope of this review to give a detailed insight into photonic devices inscribed by FLP, but we will briefly report the different strategies presented in the literature and give a more detailed view of those involving LOC applications.

Optical WGs, which can be considered as the basic building block of these photonics devices, can be easily fabricated with the femtosecond laser in materials like glasses, crystals, or polymers [26, 70]. As discussed in the previous section, the morphological effect strongly depends on the material characteristics, but thanks to the 3D nature of FLP, it is possible to play with the geometry of the irradiated region in order to obtain the higher refractive index volume needed to confine light (Figure 1).

The most straightforward technique is to find the laser conditions to obtain a refractive index increase with respect to the unmodified material. The irradiated region will define the WG core (see Figure 1A), and then by scanning the sample with the laser focus, once or several times, a channel that directly guides light through will be obtained. This strategy is the most successful to fabricate optical WGs in a multitude of vitreous materials like fused silica [52, 71, 72], borosilicates [73], phosphates [74],

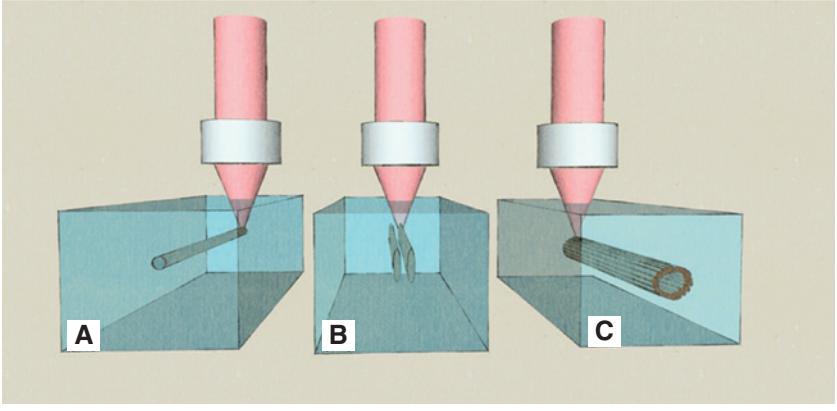

Figure 1: Schematic view of the three main geometrical architectures to obtain optical waveguides by undeformative femtosecond laser processing.
Different architectures to obtain optical waveguides by undeformative FLP, (A) the increase on the refractive index is induced in the laser focus, (B) the guiding region is defined by two damaged tracks, or (C) the guiding region is surrounded by a closed irradiated pattern.

heavy metal oxides [75], or chalcogenides [76]. There are also some examples in polymers [77] and crystals [70], but their guiding properties are not as good as for glasses.

This approach cannot be successfully implemented in those materials in which it is only possible to obtain a decrease in the refractive index, like in some glasses, or damaged regions, like in most crystals. In those cases the only way to fabricate the WGs is to inscribe with the laser the cladding in order to obtain light confinement in the bounded, nonirradiated region.

An easy strategy is to obtain the WG core between two parallel damaged lines created with the femtosecond laser (see Figure 1B). Due to the stress field induced by the irradiated tracks, there is a refractive index increase in the bounded volume that allows waveguiding. This architecture is mainly used for the fabrication of WGs in crystals, for example, in $LiNbO_3$ [78], $(BaBO_2)_2$ [79], or diamond [80] but also for ceramics such as yttrium aluminum garnet (YAG) [81] or polymers like polymethyl methacrylate [82]. Whenever that second strategy is not enough to implement good WGs, researchers have followed a third architecture by defining a closed cladding by the femtosecond laser irradiated regions (see Figure 1C). Depending on the material, it might be a depressed cladding with a lower refractive index like in ZBLAN glass [83] or a damaged pattern like for YAG crystals [84, 85].

Undeformative FLP is a powerful technique for the integration of photonics components into microfluidic devices [43, 86]. Its 3D nature allows to integrate the photonic circuits in any position inside the microfluidic chip, allowing for complicated and compact configurations [15]. Moreover, as it is a direct fabrication method (the photonic devices are fabricated in a single step by moving the sample relative to the laser beam following a desired path) it allows, for example, to integrate the photonic circuits into microfluidic devices fabricated by traditional techniques (see Figure 2).

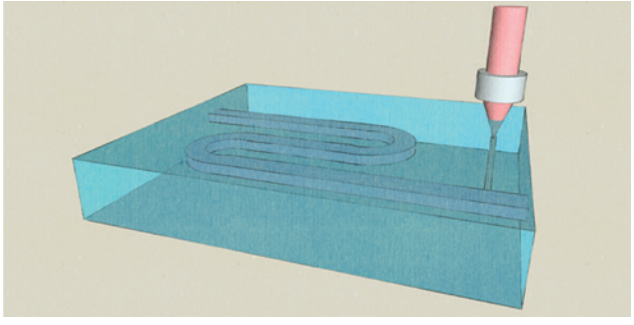

Figure 2: The high flexibility of FLP allows the integration of optical circuits into microfluidic chips fabricated with traditional techniques.

These integrated photonics circuits allow to excite, detect, and optically manipulate the biological specimens flowing through the microfluidic channels. An example consists in adding optical WGs to commercial fused silica microfluidic LOC to perform on-chip fluorescence [30] or an optofluidic switch using a ferrofluid plug [87]. Similarly, adding a MZI allows to perform label-free detection of relevant biomolecules [88]. The same scheme, adding a WG that crosses perpendicularly the microfluidic channel, is applied for the optical manipulation of samples; in fact, the light coming from optical WGs exerts optical forces that can be exploited to trap and deform cells flowing in a microchannel, thus characterizing their mechanical response [89]. These examples demonstrate the high potential of FLP in the LOC field as it allows the upgrading of traditional microfluidic devices to implement new biological and chemical experiments.

4 Subtractive processing

Subtractive FLAE is widely used to create 3D microfluidic structures in glass microchips. As a first step of FLAE, laser processing parameters such as scanning direction, speed, and laser power are adjusted to achieve desired shapes. Following a computer-aided design program, the laser irradiation is then carried out. For FLAE, two kinds of glass are available; one is a photosensitive glass, and the other one is fused silica. In case of a photosensitive glass, a critical dose, Dc, reflected in a photoreaction threshold, is important rather than the laser fluence [90, 91]. This dose is defined as the amount of photons necessary for creating a network of nuclei with appropriate density for growth of a continuous crystalline phase at the laser exposed regions which eventually induces selective chemical etching. The photosensitive glass for FLAE is represented by Foturan glass, which is composed of lithium alumino-silicate doped with traces of Ag, Ce, and Sb ions. During laser irradiation, a mechanism similar to Kreibig's evaluation for Ag containing photosensitive glasses exposed to UV light could be proposed in which latent image are obtained in glass by photoreduction of Ag ions to Ag atoms with free electrons generated by multiphoton absorption of femtosecond laser beam [92]. It was found that the photoreaction in case of 775 nm wavelength femtosecond lasers takes place by six photons process, while the critical dose, $Dc = 1.3 \times 10^{-5}$ J/cm^2 [91]. During the thermal treatment after the irradiation, precipitated Ag atoms are clustering to act as nuclei for growth of crystalline phase of lithium metasilicate at the laser exposed regions. As a result, one can visibly observe the modified

patterns as dark color inside photosensitive glass (Figure 3A, D, and G), which can generate approximately 50 times higher etching rate in diluted hydrofluoric (HF) acid solution as compared with nonlaser exposed regions. The etching time is one critical parameter in order to develop uniform channels with similar width over extended lengths (Figure 3B, E, and H). Finally, a post-thermal treatment is carried out in order to decrease the roughness from several tens of nanometers of as-etched surface to the nanometer range (Figure 3C, F, and I). The additional thermal treatment can go up the smoothening of glass and offers highly transparent samples for optical integration (Figure 3F and I). It can thus achieve microfluidic LOC platforms with unique scale-down (μm)-scale-up (mm) characteristics and robustness for easy handling.

FLAE of Foturan glass was applied to fabricate nano-aquariums for microorganisms' studies, since the surface smoothness of microfluidic channels is essential for clear observation of dynamics of the microorganisms. Specifically, it enabled 3D observation of rapid, continuous motion of flagellum of *Euglena gracilis* [93]. The nano-aquariums exhibit some advantages over the conventional observation method using a slide glass with a cover glass or a petri dish, which are the extraordinary shortened observation time and the ability of 3D observation.

Various nano-aquariums consisting of 3D microfluidic structures integrated with some functional microcomponents by FLAE have been fabricated to demonstrate that they are an effective and powerful tool for the dynamic analysis and determination of functions of living cells and microorganisms. Specifically, complex, microfluidic configurations were proposed for the elucidation of gliding mechanism of *Phormidium* in soil for vegetables growth acceleration [34]. It was found that CO_2 secreted from the seedling root attracted *Phormidium* in the presence of light. Further, the light intensity and specific wavelength necessary for gliding were determined. *Phormidium* started to glide to a seedling root when white light

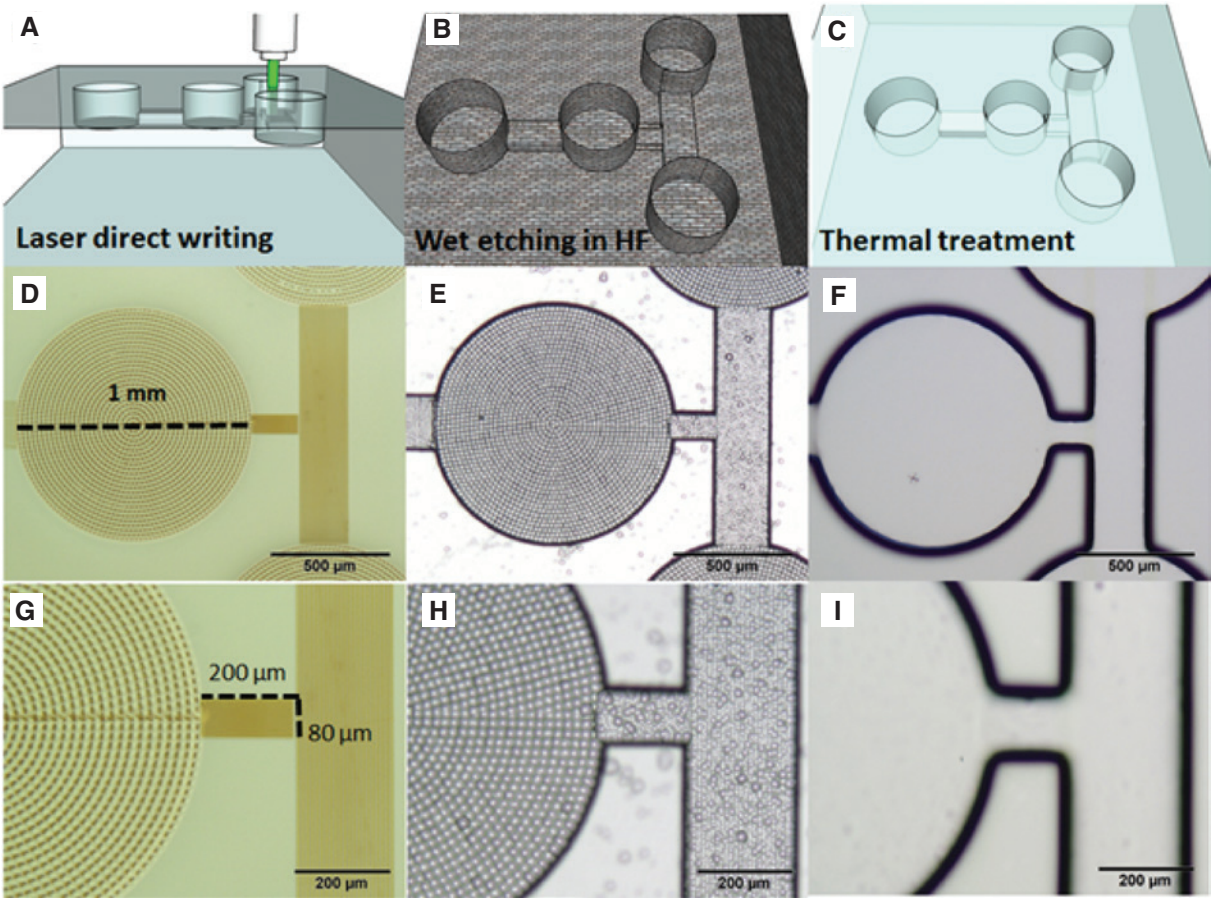

Figure 3: Schematics of FLAE process.
(A) Laser direct writing followed by first thermal treatment; (B) wet chemical etching in HF; and (C) second thermal treatment. Optical images of photosensitive Foturan glasses after exposing to fs laser irradiation followed by first thermal treatment (D and G for detail), 45 min etching in a 10% HF etching (E and H for detail) and successive post-thermal treatment for smoothening the etched surfaces (F and I for detail).

intensity was above a threshold estimated at 1530 lx. It was also revealed that red light only (640–700 nm) promoted *Phormidium* gliding. One can suppose that new methods for accelerating vegetable seedling growth can be further developed based on these findings.

Besides Foturan, fused silica was also proposed for LOC applications. Fused silica exhibits better optical performances such as broader transmission range and lower autofluorescence. In addition, after femtosecond laser writing of 3D patterns inside silica glass, fabrication of 3D microfluidic channels in volume is possible by simple etching of the laser-exposed silica in diluted HF without any thermal treatment [32]. In this case, etching selectivity originates from weakened chemical bonds induced by physical process of femtosecond laser irradiation. Foturan glass allows, however, fabricating larger scale of complex microfluidic structures due to lower laser fluence, higher scanning speed, and higher etching rate and can be thermally treated after the etching in order to obtain smooth surface with nanoscale roughness. The latter characteristic is particularly important for many applications. 3D microfluidic structures fabricated in fused silica by FLAE was proposed to be used for a 3D mammalian cell separator biochip [94]. The sorting was based on differences of cell deformability depending on cytoskeletal architectures. Specifically, T-junction configurations and microchannels with narrow constrictions could function as filters for sorting by a pressure-driven flow control (Figure 4A). This resulted in cell deformation by the pressure gradient maintained across the constrictions and further guidance towards outlet. Rigid cells that could not pass constrictions were guided to a second outlet. It was also evidenced that during cell sorting, the cell population maintained cellular integrity (Figure 4B).

Another application of FLAE of fused silica was a 3D hydrodynamic focusing microfluidic device [95]. This proves the microfabrication capability of interconnecting microchannels in 3D to demonstrate two-dimensional (2D) hydrodynamic focusing, in horizontal or vertical plane, or full 3D hydrodynamic focusing. The device consisted of two inlets for the sample flow and for dividing into four microchannels for producing the sheath flows. By individual control of the pressures only, the biochip allows 3D symmetric flow confinement to count cells/particles at a very small area near the center of the channel.

Very complicated microcoils with large aspect ratios were fabricated by FLAE [96]. Long microchannels with high uniformity for microcoil applications were achieved, demonstrating the flexibility and controllability in fabrication of 3D complex structures. The two steps of manufacturing process, 3D microchannels fabrication and injection with metal gallium into the fused silica channels, are schematically shown in Figure 5-I along with optical images of etched and injected microchanels (Figure 5-II).

Such structures can be proposed for microelectric systems in which U-shaped and O-shaped inductances with special magnetic field distributions can efficiently serve as biological sample testing, cell filtration, or particles trapping.

FLAE was extended to fabrication of microfluidic structures in other materials. Hollow microfluidic channels embedded in the Nd:YAG crystal reveals the potential of fabricating new optofluidic devices in optical gain materials [97]. It is supposed that femtosecond laser pulses locally modify the crystalline state inside Nd:YAG network producing bonds braking and micro-cracks. When material is introduced in orthophosphoric acid baths at elevated temperatures, the laser exposed regions allow a faster acid penetration inside YAG crystal than

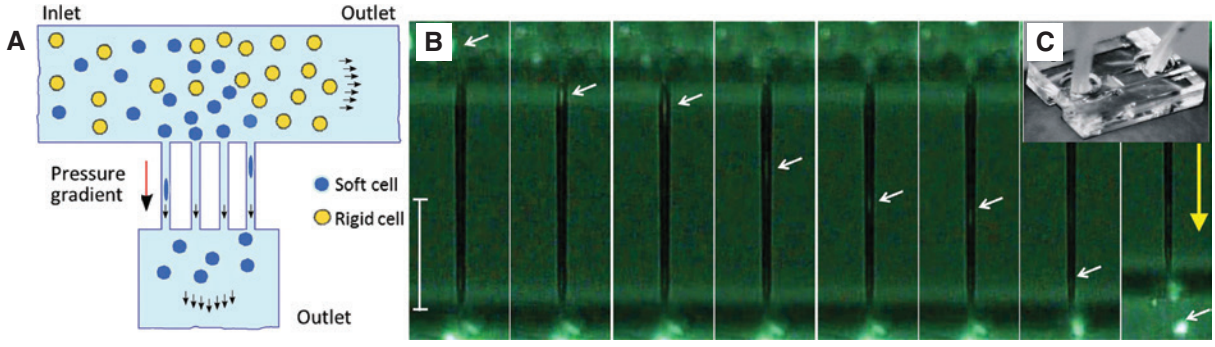

Figure 4: Biochip device for cell sorting.
(A) Schematic of working mechanism of the cell sorting device: a pressure gradient applied between two microchannels allows softer cells to squeeze through the constrictions and be collected at outlet 1; (B) fluorescence images of a deformed single cell traveling through channel constrictions. The scale bar represents 100 μm, white arrows show positions of the cells, yellow arrow indicates flow direction, and (C) magnified optical image of a fingertip size LOC device. Reproduced from [94] with permission from Royal Society of Chemistry.

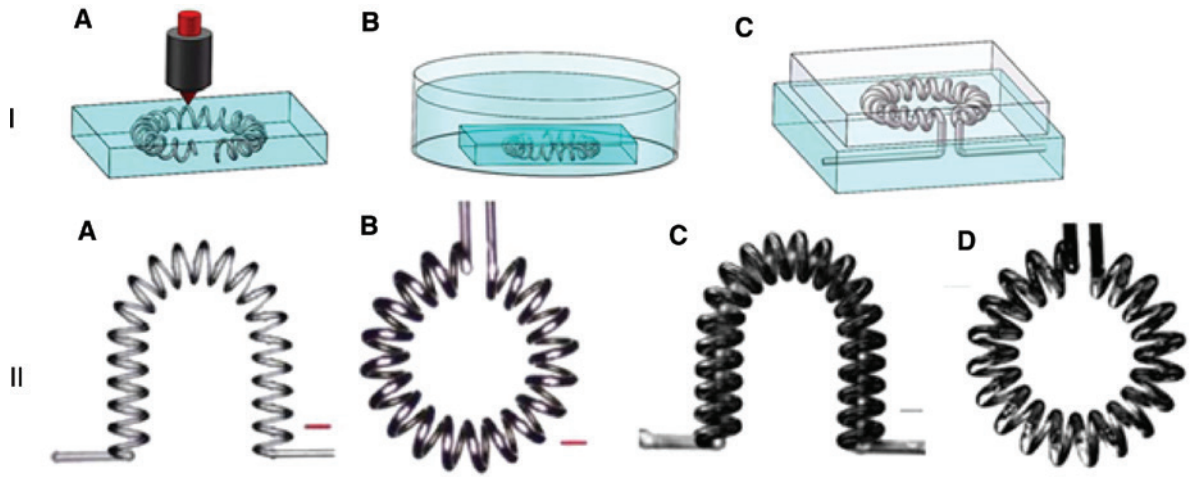

Figure 5: 3D microcoils filled with metal gallium in fused silica.
I. Schematics of the two-step fabrication process: (A) laser modification, (B) HF etching, (C) microsolidify process and II (A) U-shaped etched microchannel, (B) O-shaped etched microchannel, (C) U-shaped inductance injected with metal gallium. (D) O-shaped inductance injected with metal gallium. The scale bar equals 100 μm. Reproduced from [96] with permission from Optical Society of America.

unexposed zones and thus developing the embedded microchannels. Besides glass, 3D microfluidic channels were fabricated in a fluoric polymer called CYTOP® by subtractive manufacturing [98]. In this case, femtosecond laser is also followed by wet etching using a specific fluorinated solvent and annealing in order to develop embedded channels inside the polymer. Such biochips allowed a clear observation of flagellum motion of dinoflagellates, species belonging to marine eukaryotes, since refractive index of CYTOP is almost the same as that of water. Laser-assisted subtractive fabrication of complex 3D structures was achieved even in silicon (Si) by using laser pulses at a wavelength of 1.55 μm, duration of 5 ns, and repetition rate of 150 kHz [99]. The process is based on nonlinear feedback mechanisms arising from the interaction of infrared laser pulses inside Si [100]. The laser-modified Si patterns have a different optical index to that of unmodified parts. A focused laser beam passes through the Si, while a third of it is reflected back from surface due to Fresnel reflection and propagates along with incident beam (Figure 6A). By using additional pulses, their focal points shift along optical axis and modify the material, changing the optical path of the subsequent pulse. The irradiated region gradually gets longer while keeping its aspect ratio beyond the diffraction limit (Figure 6B). These modified parts can be chemically etched in a solution consisting of $Cu(NO_3)_2$, HF, HNO_3, and CH_3COOH to produce desired complex 3D shapes (Figure 6C and D). A large spectrum of possible applications of such buried microfluidic channels is then expected since the silicon is an excellent material for microelectronics as well as integrated photonic platforms.

Another subtracting laser method for fabrication of 3D glass microfluidic structures is WAFLD. In this technique, the glass is immersed in water and ablated from the rear surface to the volume by focused femtosecond laser beam in order to create 3D hollow structures [101]. In this process, the water plays the role of removing the eventual debris from the laser-ablated regions during drilling. Long channels with 3D complex structures can be thus fabricated [102, 103]. An issue of the method is the femtosecond laser-induced debris which can clog the channel during drilling and restricts the length of the fabricated channels to ~1 cm. Then, femtosecond laser direct-write ablation of porous glass immersed in water followed by post-annealing has been proposed to overcome the issue [36].

5 Additive processing

In laser-based additive manufacturing (AM) processes, light is used to build 2D or 3D objects by depositing material, such as plastic, ceramics, metal, or even biomaterials onto a solid substrate; the size range of the end product varies from submicrometer to centimeters. Laser AM processes can be classified in various ways [104]; in this section we concentrate on the FLP [105, 106] with special attention to their microfluidic application. The application of femtosecond lasers for AM takes advantage of the multiphoton processes described earlier where the focused beam affects only a very small spatial element; this results in complex 3D objects with submicrometer feature size

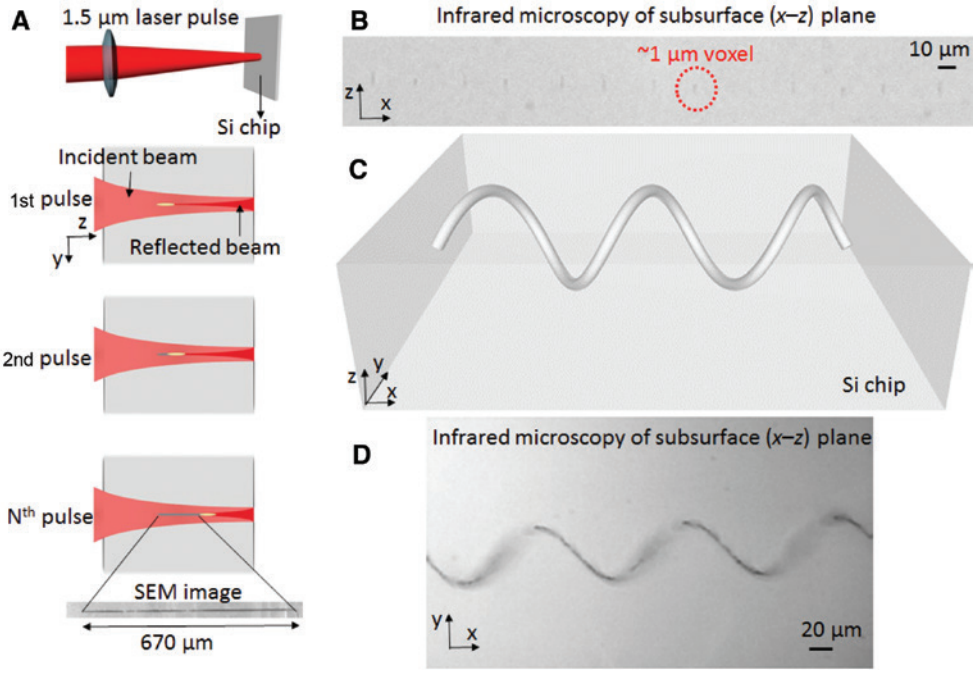

Figure 6: 3D helix inside Si chip.
(A) Schematic of laser pulses interaction with Si chip. The laser pulse collapses and modifies the local Si crystal structure. Consecutive laser pulses focus to shifted positions, axially elongating the structured region. Inset: scanning electron microscopy (SEM) image of a rod-like structure in Si. (B) Infrared image of an array of 1-µm-sized voxels, each created by a single laser pulse, (C) design of an in-chip 3D structure, and (D) Infrared image of a 1-µm-thick, 1-mm-long helix by point-by-point fabrication. The scale bars equal 10 and 20 µm. Reproduced from [99] with permission from Nature Publishing Group.

even deep inside the sample. Since FLP, except for a few examples, uses focused laser beam, it is mostly scanning processes: the focus translates along a pre-defined trajectory relative to the sample.

The possibility of creating highly conductive metal interconnections of micrometer dimensions, especially in 3D inside microfluidic channels, promotes intensive research in FLP of metals. Techniques such as selective laser melting, photoreduction, or selective electroless plating have already been introduced [107–110]. Micrometer-sized metal wires of smooth surface and high conductivity was made with femtosecond laser photoreduction of silver nitrate by Maruo and co-workers [107]. They mixed Ag-nitrate with the ethanol solution of polyvinylpyrrolidone, dried it into a thin film on a glass substrate, and illuminated with a 200 fs laser of $\lambda = 752$ nm. Continuous silver lines of 0.2–1.7 µm width and 0.1 µm thickness were made with the resistivity of 3.48×10^{-7} Ωm, only 22 times larger than that of bulk silver. Microfluidic integration of metallic interconnections and electrodes were shown by Xu and co-workers [109, 110] using femtosecond laser-assisted electroless metal plating. The walls of a microfluidic channel, fabricated with the FLAE process, were roughened by femtosecond laser illumination on distinct areas. Electroless plating was selective for the rough surfaces; the resistivity of the deposited gold layer was only 1.9 times larger than that of bulk gold. This highly conductive gold layer was used in a microfluidic channel as micro heater and as electrodes for the orientation of the elongated microorganism *E. gracilis* using high-frequency AC electric field. Highly conductive structures can also be prepared involving TPP in which the composite photoresist contains some functional filling materials. Such materials can be metal salts that reduce to atomic metals during the TPA or the polymerization process. Shukla and co-workers used a gold chloride filling material to prepare conductive polymer lines of 800 nm width achieving conductivity a quarter of that of bulk gold this way [111]. Further, carbon nanotubes (CNT) are also a promising filling material to fabricate conducting polymer structures. Xiong and co-workers achieved the alignment of CNTs inside the polymer matrix and fabricated polymer structures with conductivity of 10^2 S/m only when the CNT were parallel to the polymerized lines; the use of CNT also improved the structures' mechanical characteristics [112]. TPP of these composite materials will be sure to further enrich functionality of LOC devices.

The preparation of polymer microstructures with femtosecond lasers is based on the multiphoton absorption of the material; therefore, this process is also called

multiphoton polymerization (MPP); in the vast majority of the cases it means TPP. Photoresists for TPP must contain at least two functional ingredients: the monomer and a photoinitiator. The broad range of photoresist monomers include epoxy- and acrylic-based ones, but organic-inorganic materials are very popular too [113]; recently biomaterials have also been introduced [114]. TPP uses a single focused laser beam which needs to be translated relative to the sample in three dimensions (direct laser writing) (Figure 7A) [37]. To extend the high-resolution structures, this scanning process can be quite time consuming, so that it is desirable to speed it up considerably for practical reasons. Two main directions evolved to achieve this are the following: in the first, the process is parallelized by multiplying the single beam optically using microlens arrays [116], kinoforms [117], or spatial light modulators (SLMs) [118], but distributed intensity pattern can also be created [119]. The second way is to increase the scanning speed of the focus over the extended area. In the early TPP papers a few tens of micrometer-per-second scanning speeds were applied, but recently millimeter-per-second velocities were already realized by moving the sample with high-precision air-bearing 3D stages [120] or by scanning the focal spot with a pair of galvo-scanned mirrors, available already in commercial TPP units [121]. Such fast scanning on the other hand requires elevated laser power and the advancement of the photoinitiator molecules [122]. The size of the smallest detail on a 3D structure that can be made with TPP structure (feature size) is typically around 150–200 nm, but with various deactivation methods feature size of <50 nm was demonstrated even in the axial direction [61, 123, 124]. With this value TPP can today approach the resolution of e-beam lithography while maintaining the benefit of producing 3D structures in one step.

The integration of micro-optical parts made by MPP inside microfluidic chips is extensively investigated and promises great potential in micro-imaging, beam shaping, or sensorics. Photonic crystals (PhC) offer peculiar optical characteristics, with tailor-made transmittance or reflectance spectrum [115, 125]. Serbin and co-workers prepared woodpile PhCs (Figure 7B) with transmission windows in the 1.2–1.6 μm wavelength region (Figure 7C). The transmission window was shifted down to ~470 nm with a stimulated emission depletion (STED)-like polymerization scheme capable of preparing woodpile rods of 120 nm thickness with 300 nm spacing [61]. Complex PhCs can also be prepared with a single illumination using interferometric methods [119]. Haque and co-workers [126] integrated PhCs with microfluidics by polymerizing woodpile structures inside a quartz channel to use as a capillary electrophoresis system; the PhC structure served as the stationary phase of a chromatographic column. The detectable optical signal originates from the PhC's stop band shift when the analyte, bound to the PhC, changes its refractive index.

Microlenses are probably the most important micro-optical elements to be integrated into a microfluidic channel for their light focusing or imaging capabilities. Simple spherical lenses [127] and concave-convex lenses with improved imaging and focusing performance [128] were already developed. Micro-optics was also polymerized on the tip of single-mode fibers for microfluidic applications: light was focused, collimated, or shaped into exotic intensity distribution this way [129, 130]. Wu et al. [48] integrated a series of spherical lenses with a guiding wall system into a microfluidic chip prepared with the FLAE method (Figure 7D). Seven lenses were arranged across a 280 μm wide microfluidic channel focusing white light with them; cells were introduced

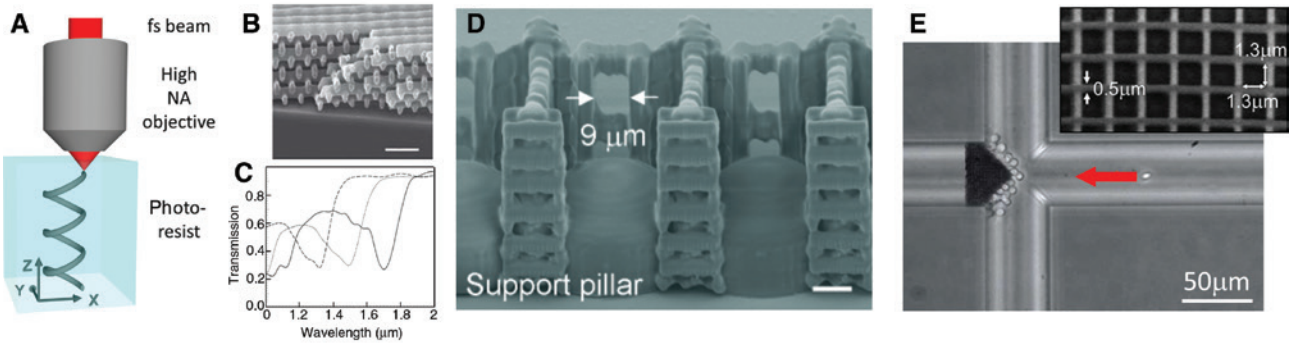

Figure 7: Schematics of, and structures made with two-photon polymerization.
Schematics of the TPP method (A). SEM image of a log-pile PhC structure (B) and transmission spectra of the PhC with rod spacings of 1.0 μm (solid line), 0.9 μm (dotted line), and 0.8 μm (dashed line) (C). Adapted by permission from Macmillan Publishers Ltd: [115] copyright (2004). SEM image of the cell counter equipped with microlenses and aligning walls (D). Scale bar: 10 μm. Reproduced from [48] with permission from the Royal Society of Chemistry. Cleanable structure filtering red blood cells form a suspension in a microchannel (E); the insert shows the pore size of the filter.

to the channel, and when a cell passed over a lens, the light intensity focused by that lens dropped considerably and the cell was counted. The guiding walls did not allow the cells to randomly pass the lenses but over their centers, maximizing the intensity change of the detected light; 100% cell counting efficiency was realized this way. Besides spherical lenses, Fresnel zone planes (FZP) are a promising alternative. Their main advantage is their flatness, which enables more optimal integration into space-confined microchannels [131]; their focusing efficiency, in principle, can be as high as 95%. Wu and his co-workers [132] integrated FZPs into a microfluidic chip and demonstrated its imaging capabilities.

Separation of microparticles, such as cells, based on their size or shape inside microfluidic chips has a great relevance in basic research or diagnostics. The simplest, sieve-type passive filters were prepared by the Sun group [133] and Xu and his co-workers [134] as single walls with holes of various sizes. A more complex and finer filter structure with 3D can add extra functionality to the filters [40]. Amato and co-workers prepared such filter as a log-pile structure with pore sizes ranging from 0.5 µm to 3 µm inside of a microfluidic channel (Figure 7E). Microbeads were filtered in two characteristic situations: (i) small amount of sample is filtered for a long time and (ii) most of the samples are filtered as fast as possible. One remarkable feature of this filter is that it can be cleaned with a reverse flow and re-used several times. Arc-shaped filter that can distinguish and capture particles in three size ranges was just recently presented [135]; the flow around the filter can also be reversed, allowing the collection of the captured particles.

Mixing and pumping solutions in the pico- and femtoliter scale, typical in microfluidic systems, is also a sought after task that tailor-made microtools can efficiently solve. A passive mixer was implemented in the form of tune bundles in the vertical and horizontal directions to split and realign segmented streams of the laminar flow [136]; 94% of mixing ratio was achieved. Active mixing requires a driving mechanism for the tools, which very often uses light [137]. Kelemen and co-workers produced a supporting structure-stabilized, freely rotating microgear that rotates with 2 Hz with the potential for using it as a mixer [138]. The entire rotor was integrated with a light guide also polymerized on the same cover slide. Light emitted by the light guide hits the microgear asymmetrically and induces its rotation due to scattering from its surface. Optical tweezers-assisted pumping was demonstrated by the group of Gluckstad, with the added ability to pick up and transfer microparticles [139]; their tool consisted of four spheroids for optical trapping and a tube with two openings, one of which is metallized and serves as a heating element to give rise to convective flow. Flow can not only be generated but also measured with polymer microtools; a drop shape meter connected to an axis with a thin rod spring was prepared inside the microchannel operating in the range of 1–5 µl/min flow rate [140].

Actuation of polymerized microstructures with holographic optical tweezers (HOT) has the potential of precise maneuverability and probing [141]; this tool uses multiple trapping sites in 3D created by an SLM. Mobile light guides were prepared out of the photoresist SU8 by Palima et al. [142] with the goal of redirecting light perpendicularly to the optical axis of the trapping objective (Figure 8A). The structure consisted of a bent light guide and four elliptical handles for the four trapping focal spots of the optical tweezers. Light that was shone on the entrance of the fiber parallel to the optical axis was emitted perpendicularly

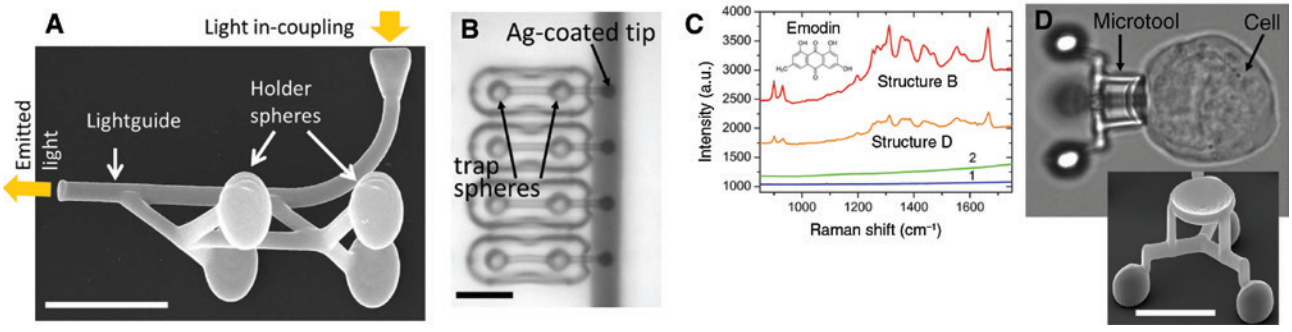

Figure 8: Optically manipulated mobile microtools to be used in microchannels.
SEM image of a mobile light guide for off-axis fluorescence excitation (A) [142]. Optical microscopy image of four Ag nanoparticle-coated microtools used for SERS measurements (B). Raman spectra of emodin as measured with the Ag-coated structures (structure B and structure D), in the bulk solution (spectrum 1) and with an uncoated structure (spectrum 2) (C). Reprinted with permission from Vizsnyiczai et al. [143]. Copyright (2015) American Chemical Society. Optical microscopy image of an indirectly manipulated K562 cell using a polymerized microtool that is held and actuated with HOT (D); the insert shows the SEM image of the microtool [144]. All scale bars are 10 µm.

to the original direction; this light can be used for localized fluorescence excitation at the side of a cell, from a direction not accessible otherwise. The positioning accuracy was demonstrated by selectively excite-stacked fluorescent beads of 3 μm diameter. In a similar work, an optically actuated polymer structure was used in a microfluidic channel to facilitate surface-enhanced Raman spectroscopy (SERS) [143]. Here, the microstructure had a probe part with a tip and two spheroid parts for the optical tweezers (Figure 8B). The tip was coated with silver nanoparticles of 20–160 nm diameter; such nanoparticles are known to enhance Raman scattering. Inside of a microfluidic channel, SERS signal of emodine, an anticancer drug, present only in 10^{-6} M concentration, was detected only when Raman signal was collected from the Ag-coated tip (Figure 8C).

Optically actuated, two-photon polymerized mobile structures can also manipulate single cells. Asavei and co-workers prepared a paddle wheel to create shear force with rotation in the close vicinity of cell membranes [145]. A HOT can hold it, and the rotation was driven by a third beam, illuminating the paddles directly. The liquid flow around the rotating paddles was modeled with hydrodynamic simulations, showing a moderate generated drag-torque. In the second work polymerized microstructures were used to actuate single, nonadherent cells with 6 degrees of freedom. In this indirect manipulation scheme, the cells were attached to the structures biochemically, and the actuation was realized again by a HOT [144, 146]. The microtool consisted of three spheroids where the optical tweezers can trap it and a disk-shaped part to which the cell can bind (Figure 8D). The microtool was designed such that the attached cell avoided the high intensity trapping beams, while high optical forces could precisely hold the structure in place [144]. The cells could be translated and rotated with up to 50 μm/s and up to 65°/s, respectively.

Two-photon polymerized scaffold structures to study various aspects of cell growth are extensively studied. This artificial support has to mimic the extracellular matrix (EM) of the cell that provides them structural integrity and influences their metabolism. Log-pile scaffold structure was prepared from the biocompatible ORMOCER resin by Weiss and co-workers [147, 148] to study how bovine chondrocyte cells inhabit such structures; they found that the cells could only infiltrate the structure with pore size above 60–70 μm. Guided growth of nerve cells (NG108-15 and PC12 cell lines) were studied on polylactide scaffolds [147], and it was found that linear structures promote directed cell growth and PC12 cells can make interconnections with cells grown on neighboring structures. The material of the scaffold also has a crucial role in cell growth. Klein and co-workers [149] prepared a scaffold structure of polyethylene glycol diacrylate (PEG-DA), a cell-repellent material and of the biocompatible ORMOCOMP (Figure 9A). On the 3D PEG-DA support small ORMOCOMP cubes were polymerized at selected locations. It was found that fibronectin, an EM protein, binds preferentially to ORMOCOMP and that chicken fibroblast cells cultured on the scaffold adhered to the fibronectin-coated nonplanarly arranged ORMOCOMP cubes (Figure 9B); it demonstrated the possibility of 3D control of cell growth and shape. Recently, biomaterials are also used directly to create 3D structures with femtosecond lasers. In these approaches [150] the illumination of a protein solution mixed with a photoinitiator results in a crosslinked protein matrix forming a stiff 3D structure; bovine serum albumin was used as structural

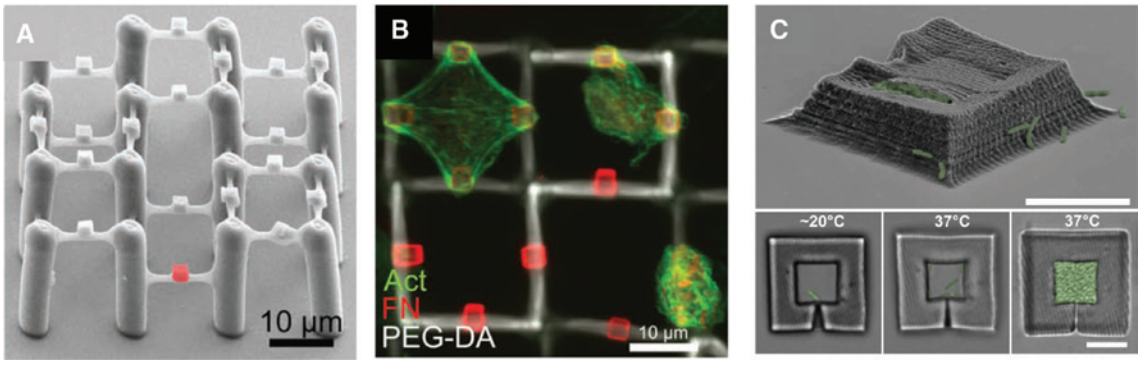

Figure 9: Static polymerized microstructures for biological applications.
SEM image of a 3D scaffold to study cell growth; the supporting structure is made of PEG-DA, the attached cubes of ORMOCOMP (A) [149]. Chicken fibroblast cells preferentially attaching onto the ORMOCOMP cubes (B). Adapted from [40] with permission of the Royal Society of Chemistry. Chambers made of bovine serum albumin to study bacterial behavior (C) [114]. Scale bars: 10 μm.

material for bacterial traps (Figure 9C) [114] or chitosan for scaffolds for cell growth [151].

6 Hybrid processing

Combination of different schemes of 3D-FLP can further enhance functionalities of LOCs. The typical approach is the undeformative femtosecond laser direct writing of optical WGs and WG-based photonic components (such as MZI) in 3D microfluidic devices fabricated by subtractive FLAE. For example, a functional device based on fused silica was proposed for single-cell detection [152]. For detection of a single red blood cell (RBC) in diluted human blood filled inside the glass microchannel, two interrogation approaches were proposed: (i) intensity change of the He-Ne laser light delivered by a WG due to refractive-index difference of a flowing cell and a liquid medium and (ii) detection of fluorescence emission from dyed RBCs when excited with Ar laser light delivered by the WG. In another study fluorescence detection and successive sorting of a single cell were implemented by WG-integrated optofluidic devices in fused silica [153]. The X-shaped channel design consisted of two inlet channels merging in a center straight channel in which fluorescence detection and sorting were successively applied. The target cell was detected by fluorescence using the laser beam delivered from fluorescence WG. When the specific fluorescence signal from the target cell or particle was detected, the optical force laser beam was switched on to guide it to the channel by the sorting WG with a suitable delay time. As a result, the optical force laser beam pushed the target cell into the buffer solution to eventually sort it out in the desired outlet channel. The device was able to investigate only a limited number of cells while keeping a high sorting selectivity. Integration of Bragg grating waveguides (BGW) in different optofluidic device geometries were proposed (Figure 10) in order to improve sensor efficiency [154]. Writing the BGWs very close to the microchannel enabled an evanescent probing of the WG mode into the liquid-filled channel for refractive index sensing in the range from 1 to 1.452 with high sensitivity.

Such BGW sensors integrated into 3D LOC devices for optofluidic sensing were proposed for chemical synthesis and monitoring of biomolecular interactions.

Another hybrid scheme to enhance the functionalities of LOCs is a combination of subtractive and additive 3D-FLP. Integration of micro-electric components in 3D

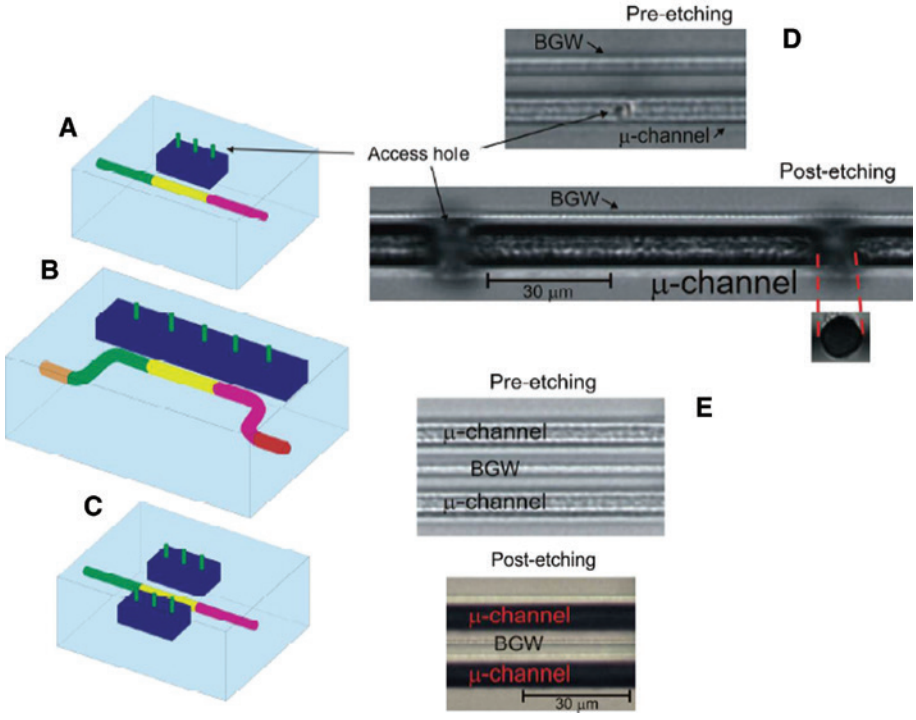

Figure 10: Microfluidic sensor with different geometries: straight BGW with a single channel (A), S-bent BGW with a single channel (B), and straight BGW with double channels (C).
Optical images before [top pictures in (D) and (E)] and after [bottom pictures in (D) and (E)] HF etching for sensor designs of the straight BGW with a single channel (D) and the straight BGW with double channels (E). Reproduced from [154] with permission from Optical Society of America.

microfluidic glass channels by femtosecond laser selective metallization was demonstrated for electrical control of biological samples. This technique involves subtractive FLAE and successive additive process of space-selective metallization of glass microfluidic structures in which femtosecond laser direct-write ablation followed by electroless metal plating is implemented [155]. It was found appropriate for flexible coating with metal films into desired locations inside 3D microfluidic structures. It was then applied to integrate two opposed microelectrodes in a straight microfluidic channel to align the swimming direction of asymmetric biological samples such as *E. gracilis* based on electro-orientation nature.

Hybrid subtractive-additive femtosecond laser microfabrication consisting of ablation, TPP, and welding was recently proposed for LOC fabrication using an identical Yb:KGW femtosecond laser source [156]. In a first step, laser ablation was employed to fabricate microfluidic channels in glass substrates. Then, by 3D lithography, microfilters were integrated into the channels. In a final step, the chip was closed by a glass cover using laser welding. The LOC device with microfilters was fabricated for sorting 1 to 10-μm diameter microparticles in water.

Alternative hybrid subtractive and additive 3D-FLP is known as ship-in-a-bottle integration, in which subtractive FLAE of glass is followed by additive TPP of negative photoresists in order to fabricate hybrid inorganic-organic LOC devices with polymeric 3D microstructures possessing specific functionalities in embedded glass microfluidic channels. LOCs fabricated by this novel technique can then be called "ship-in-a-bottle" biochips. Using it, one can lower the sizes of various 3D complex objects developed inside channels down to the dimensions below 1 μm, while improving the structure stability and offering robustness after assembling. The capability of laser beams to directly fabricate 3D desired shapes of both glass channels and polymeric patterns allows to customize the design of 3D biochips for concrete applications.

One of the advantages of hybrid subtractive and additive 3D-FLP is ability of fabricating "ship-in-a-bottle" biochips using the same femtosecond laser setup. One could thus exploit specific advantages of each process while diminishing the drawbacks. Both the glass and polymers are transparent materials, both of which have great potential for biochip applications. By the hybrid laser technique, the sizes of detailed structures inside the glass microfluidic channel can be reduced as much as below the level of single-cell dimensions at which individual cells can be influenced and manipulated inside the glass channel. Such biochips can thus allow exploring phenomena at cellular levels with submicron resolution representing an excellent opportunity to get more insights on biological aspects. Totally transparent microfluidic and optofluidic biochips based on the glass microfluidic devices integrated with 3D polymer microcomponents can build suitable 3D microenvironments to study living microorganisms and to improve cell detection or sorting. In addition, a great potential is foreseen for manufacturing appropriate biomimetic structures for specific cellular analyses.

The hybrid processing technology began by applying FLAE to a photosensitive glass for the fabrication of 3D glass microfluidic structures. TPP was then applied to a negative epoxy-resin injected into the fabricated glass microchannels.

Functional biochips fabricated by the hybrid technique were already proposed for some specific applications. Specifically, a multi-functional filter-mixer consisting of two filtering sheets placed at the inlet and outlet of a passive type mixer was grown inside a microfluidic glass channel [46]. A configuration consisting of layered crossing tubes guided the flow and allowed fast mixing in a short channel distance. The integration of such a multifunctional microcomponent inside a Y-shaped closed glass channel permitted an excellent mixing performance of two fluids with an efficiency of about 87% with filtering large particles. Another functional biochip fabricated by the hybrid technique represented an optofluidic platform consisting of 3D microlens array integrated with center pass units. The device was used for parallel *Euglena* cell counting by monitoring intensity changes induced by *Euglena* cells swimming through center pass units and above microlenses [48, 157].

The hybrid approach was recently applied to fabricate biomimetic environments in closed 3D glass microfluidic channels for human cell experiments [49, 158]. Specifically, sinusoidal polymeric ridges with very high aspect ratio and modulated periodicities were proposed for cellular studies. Modulated spaces in both the periodicity and amplitude of periodical sinusoidal patterns could mimic biological environment that eventually induced controlled cell migration [158]. Thus, one foresees some useful applications for cell manipulation such as guidance and orientation. Single-cell trapping and analysis are expected to be performed in small areas by using such "ship-in-a-bottle" biochips. Another application of 3D biomimetic environments with resolutions and hierarchy similar to organism assembling in a biochip was to test cancer cell migration potential [49]. By appropriate designs and fabrication of microfluidic systems, narrow spaces for the study of cancer cell migration were proposed (Figure 11). A cell platform with chemoattractant biomolecule reservoirs

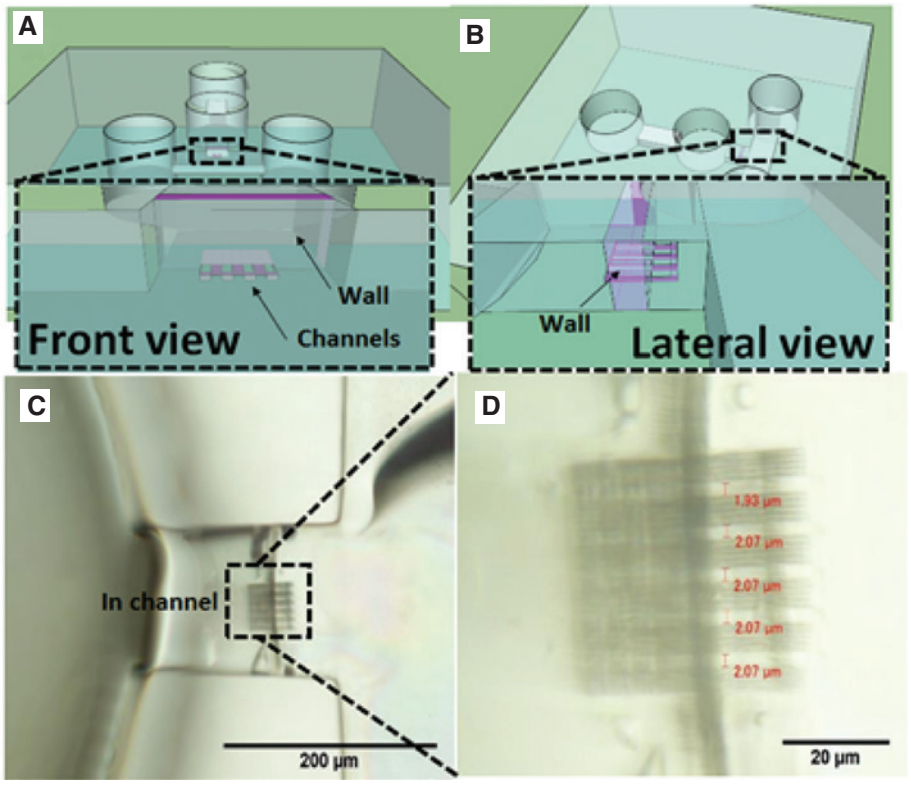

Figure 11: Schematics of, and structures made with hybrid FLAE-TPP.
Schematic of polymeric narrow channels introduced by TPP in glass microchannels (A) front view; (B) lateral view; (C) optical image of the polymeric narrow channels of 2 µm diameters and (D) detail of optical image in (C) for channel diameter evaluation.

was connected only through the polymer narrow microchannels placed at the channel base (Figure 11A and B). This configuration ensured the efficient generation of diffusion-based gradient of the chemoattractant along the submicrometric polymer channels during hours of experimental observation. Additionally, linear architecture would provide an opportunity for more insightful investigations into specific pathways controlling cancer cell migration and/or invasion. It was thus possible to take advantage of robustness of the glass biochip platform and microfluidic channel array formed using polymer in order to create very narrow spaces with 2 µm width (Figure 11C and D), which would provide similar *in vivo* environment. Such biochips could be also very useful in clinical *in vitro* trials for personalized medicine.

The hybrid FLP of both glass and polymer which can create 3D biomimetic environments with resolutions and hierarchy for organisms has enormous potential of further development. In addition, integration of optical interrogation components such as microlenses, micro-mirrors, and optical circuits for performing pump-probe experiments with laser light will greatly enhance importance in terms of the technological aspect. It is also of great interest to develop biological platforms for femtosecond lasers which offer new 3D cell culture models. The miniaturized "organs-on-chips" will allow to study human physiology in specific tissues and could replace animal testing for drug development and toxin testing. Simultaneously, the "ship-in-a-bottle" integration by TPP enables creating unique 3D tissue-like environment with submicrometer precision for cell culture in the glass platforms. Thus, these novel LOC microdevices will be applicable for high-throughput screening of small amounts of biomolecules in order to characterize human cells within the decreased dimension scale.

7 Conclusion

Lab-on-a-chip applications including microfluidic, optofluidic, and electrofluidic devices found great interest in diagnostics, environmental monitoring, chemical and biological warfare surveillance, or food industry. The main advantages of such systems are the decreased volume of the required liquid and the reduced number of molecules necessary for observation or detection allowing high-sensitivity measurements with low analyte concentrations. Besides the classically used photo- and soft-lithographic

techniques to fabricate such systems, femtosecond laser-based techniques are gaining interest due to their higher precision, broad range of target materials, and modality of usage. In this paper we review the principles of FLP and those techniques that are using such concepts for the 3D fabrication of microfluidic systems and optical and mechanical devices integrated therein.

Some of the laser fabrication techniques are regarded as undeformative processes since they modify locally only certain characteristics of the material, without removing the material itself. In most cases it means the modification of the refractive index along the illuminated path due to the stress building up in the material. Optical WGs, the basic building block of micro-photonic devices, can be easily fabricated in glasses, crystals, or polymers in an undeformative way. This allows the realization of various LOC-integrated devices such as light couplers or splitters, interferometers, Bragg-gratings, lenses, and even WG lasers. The applications include on-chip fluorescence excitation, label-free detection, and optical manipulation of the sample.

Subtractive processes were also reviewed, where the material is actually removed along the path of the laser illumination. This can be achieved either by direct ablation (WAFLD) or by chemical etching following the illumination (FLAE). Subtractive processing is used to fabricate the 3D channels or reservoirs of the LOC systems. The most popular transparent materials for this technique are photosensitive glasses, such as Foturan and fused silica. The fabrication of these materials was investigated intensively to improve the optical properties of the LOC systems; Foturan can provide good surface smoothness, while silica has broader transmission range. The major advantage of this technique is the ability to create complex 3D channel and reservoir systems in one single illumination step inside a block of the transparent material.

The femtosecond laser-based additive processes deposit 2D or 3D microstructures onto a substrate that were originally not there. The method classically includes metal deposition and TPP. The submicrometer resolution of the technique allows the integration of metal interconnections and electrodes inside a LOC system even with micrometer-sized wires and with resistivity almost that of the bulk metal. The fact that with TPP a wide range of polymer materials can be processed enables one to tailor freely the optical, mechanical, or chemical characteristics of the polymerized 3D microstructures. A new and emerging trend is the polymerization of biofunctional or biological matter, such as photocurable hydrogel structures with or without the co-addition of protein, or the protein itself into 3D structures. This holds great potential for the future use of bio-inspired materials in tissue engineering or in the fabrication of microfluidic chips to be used in diagnostic devices. The method of TPP was illustrated to allow the development of a broad spectrum of possible structures starting from micro-optical elements to cell filters and scaffolds, from liquid handling structures to those enabling optical manipulation of individual cells. Commercial TPP systems are already available, and the next great step for the research labs and also for industry could be the commercialization of such systems with the resolution-enhancement capabilities (STED-inspired TPP), which would allow further miniaturization of complex 3D devices.

The mentioned three main techniques can also be combined; the emerging hybrid fabrication techniques are taking advantage of the fact that the LOC systems can be prepared even with the same femtosecond laser system. This allows, for instance, to prepare a functional chip with a consecutive FLAE and TPP process, with FLAE and undeformative WG generation or even with the combination of the three. Such combination of techniques is holding a great potential in creating 3D biomimetic environments with the resolution of or below the single-cell level, and through the careful combination of the materials, with tailor-made functionality. All three processes can also benefit from the continuous development of beam-shaping methods that aim to enhance their efficiency or resolution by beam multiplication or specially tailored intensity distribution. The enhanced processes that use multiple focus or specially shaped intensity distribution necessitate the development of new ultrafast laser systems of considerably higher power.

Most of LOC devices currently used are still at the stage of first generation. In fact, typical LOC devices consist of monolayer microfluidic channels integrated with some functional microcomponents. In the future, increasing the degree of integration with multi-layered microfluidic systems will be required for high functionalization similar to advancement of Si integrated circuits. Three-dimensional femtosecond laser processing will be the most promising technique for fabrication of the next-generation LOC devices due to its distinct characteristics described in this article.

Acknowledgments: This work was partially supported by funding received from the CONCERT-Japan Photonic Manufacturing Joint Call (FEASIBLE project). This work has been supported in part by the GINOP-2.3.2-15-2016-00001 and the GINOP-2.3.3-15-2016-00040 programs and by the National Research, Development and Innovation Fund (grant no. NN 114692). This project has received funding from the European Union's Horizon 2020 research and

innovation programme under grant agreement No. 654148 Laserlab-Europe. This work was also supported by grant PNII-RU-TE-2014-4-1273 (187/2015).

References

[1] Mark D, Haeberle S, Roth G, Von Stetten F, Zengerle R. Microfluidic lab-on-a-chip platforms: requirements, characteristics and applications. In: Kakac S, Kosoy B, Li D, Pramuanjaroenkij A, eds. Microfluidics based microsystems. Dordrecht, Netherlands, Springer, 2010, 305–76.
[2] Figeys D, Pinto D. Lab-on-a-chip: a revolution in biological and medical sciences. Anal Chem 2000;72:330A–5A.
[3] Bashir R. Biomems: state-of-the-art in detection, opportunities and prospects. Adv Drug Deliv Rev 2004;56:1565–86.
[4] Lee S, Lee S. Micro total analysis system (μ-TAS) in biotechnology. Appl Microbiol Biotechnol 2004;64:289–99.
[5] Psaltis D, Quake SR, Yang C. Developing optofluidic technology through the fusion of microfluidics and optics. Nature 2006;442:381.
[6] Monat C, Domachuk P, Eggleton B. Integrated optofluidics: a new river of light. Nat Photonics 2007;1:106–14.
[7] Wu C-Y, Liao W-H, Tung Y-C. Integrated ionic liquid-based electrofluidic circuits for pressure sensing within polydimethylsiloxane microfluidic systems. Lab Chip 2011;11:1740–6.
[8] Liu M-C, Shih H-C, Wu J-G, et al. Electrofluidic pressure sensor embedded microfluidic device: a study of endothelial cells under hydrostatic pressure and shear stress combinations. Lab Chip 2013;13:1743–53.
[9] Yager P, Domingo GJ, Gerdes J. Point-of-care diagnostics for global health. Annu Rev Biomed Eng 2008;10:107–44.
[10] Whitesides GM. The origins and the future of microfluidics. Nature 2006;442:368.
[11] Sia SK, Whitesides GM. Microfluidic devices fabricated in poly (dimethylsiloxane) for biological studies. Electrophoresis 2003;24:3563–76.
[12] Manz A, Eijkel JC. Miniaturization and chip technology. What can we expect? Pure Appl Chem 2001;73:1555–61.
[13] Craighead H. Future lab-on-a-chip technologies for interrogating individual molecules. Nature 2006;442:387–93.
[14] Grier DG. A revolution in optical manipulation. Nature 2003;424:810.
[15] Osellame R, Hoekstra HJ, Cerullo G, Pollnau M. Femtosecond laser microstructuring: an enabling tool for optofluidic lab-on-chips. Laser Photon Rev 2011;5:442–63.
[16] Abgrall P, Gue A. Lab-on-chip technologies: making a microfluidic network and coupling it into a complete microsystem – a review. J Micromech Microeng 2007;17:R15.
[17] Liu L, Jin M, Shi Y, et al. Optical integrated chips with micro and nanostructures for refractive index and sers-based optical label-free sensing. Nanophotonics 2015;4:419–36.
[18] Bates KE, Lu H. Optics-integrated microfluidic platforms for biomolecular analyses. Biophys J 2016;110:1684–97.
[19] Breckenridge MT, Egelhoff TT, Baskaran H. A microfluidic imaging chamber for the direct observation of chemotactic transmigration. Biomed Microdevices 2010;12:543–53.
[20] Irimia D, Toner M. Spontaneous migration of cancer cells under conditions of mechanical confinement. Integr Biol 2009;1:506–12.
[21] Bhatia SN, Ingber DE. Microfluidic organs-on-chips. Nat Biotechnol 2014;32:760–72.
[22] Chichkov BN, Momma C, Nolte S, Von Alvensleben F, Tünnermann A. Femtosecond, picosecond and nanosecond laser ablation of solids. Appl Phys A 1996;63:109–15.
[23] Schaffer CB, Brodeur A, Mazur E. Laser-induced breakdown and damage in bulk transparent materials induced by tightly focused femtosecond laser pulses. Meas Sci Technol 2001;12:1784.
[24] Gattass RR, Mazur E. Femtosecond laser micromachining in transparent materials. Nat Photonics 2008;2:219–25.
[25] Sugioka K, Cheng Y. Femtosecond laser three-dimensional micro-and nanofabrication. Appl Phys Rev 2014;1:041303.
[26] Osellame R, Cerullo G, Ramponi R. Femtosecond laser micromachining: photonic and microfluidic devices in transparent materials. Vol. 123, New York, Springer Science & Business Media, 2012.
[27] Wang H, Zhang Y-L, Wang W, Ding H, Sun H-B. On-chip laser processing for the development of multifunctional microfluidic chips. Laser Photon Rev 2017;11:1600116-n/a.
[28] Sugioka K, Cheng Y. Ultrafast lasers – reliable tools for advanced materials processing. Light Sci Appl 2014;3: e149.
[29] Sugioka K. Progress in ultrafast laser processing and future prospects. Nanophotonics 2017;6:393–413.
[30] Vazquez RM, Osellame R, Nolli D, et al. Integration of femtosecond laser written optical waveguides in a lab-on-chip. Lab Chip 2009;9:91–6.
[31] Sugioka K, Cheng Y. Femtosecond laser processing for optofluidic fabrication. Lab Chip 2012;12:3576–89.
[32] Marcinkevičius A, Juodkazis S, Watanabe M, et al. Femtosecond laser-assisted three-dimensional microfabrication in silica. Opt Lett 2001;26:277–9.
[33] Bellouard Y, Said A, Dugan M, Bado P. Fabrication of high-aspect ratio, micro-fluidic channels and tunnels using femtosecond laser pulses and chemical etching. Opt Express 2004;12:2120–9.
[34] Hanada Y, Sugioka K, Shihira-Ishikawa I, Kawano H, Miyawaki A, Midorikawa K. 3D microfluidic chips with integrated functional microelements fabricated by a femtosecond laser for studying the gliding mechanism of cyanobacteria. Lab Chip 2011;11:2109–15.
[35] Liao Y, Song J, Li E, et al. Rapid prototyping of three-dimensional microfluidic mixers in glass by femtosecond laser direct writing. Lab Chip 2012;12:746–9.
[36] Liao Y, Ju Y, Zhang L, et al. Three-dimensional microfluidic channel with arbitrary length and configuration fabricated inside glass by femtosecond laser direct writing. Opt Lett 2010;35:3225–7.
[37] Maruo S, Nakamura O, Kawata S. Three-dimensional microfabrication with two-photon-absorbed photopolymerization. Opt Lett 1997;22:132–4.
[38] Stratakis E, Ranella A, Farsari M, Fotakis C. Laser-based micro/nanoengineering for biological applications. Prog Quant Electron 2009;33:127–63.
[39] Farsari M, Chichkov BN. Materials processing: two-photon fabrication. Nat Photonics 2009;3:450–2.
[40] Amato L, Gu Y, Bellini N, Eaton SM, Cerullo G, Osellame R. Integrated three-dimensional filter separates nanoscale from microscale elements in a microfluidic chip. Lab Chip 2012;12:1135–42.

[41] Liu Y-J, Chen P-Y, Yang J-Y, et al. Three-dimensional passive micromixer fabricated by two-photon polymerization for microfluidic mixing. Sens Mater 2014;26:39–44.
[42] Wu D, Wu S-Z, Niu L-G, et al. High numerical aperture microlens arrays of close packing. Appl Phys Lett 2010;97:031109.
[43] Sugioka K, Xu J, Wu D, et al. Femtosecond laser 3D micromachining: a powerful tool for the fabrication of microfluidic, optofluidic, and electrofluidic devices based on glass. Lab Chip 2014;14:3447–58.
[44] Gross S, Withford M. Ultrafast-laser-inscribed 3D integrated photonics: challenges and emerging applications. Nanophotonics 2015;4:332–52.
[45] Osellame R, Maselli V, Vazquez RM, Ramponi R, Cerullo G. Integration of optical waveguides and microfluidic channels both fabricated by femtosecond laser irradiation. Appl Phys Lett 2007;90:231118.
[46] Wu D, Wu SZ, Xu J, Niu LG, Midorikawa K, Sugioka K. Hybrid femtosecond laser microfabrication to achieve true 3D glass/polymer composite biochips with multiscale features and high performance: the concept of ship-in-a-bottle biochip. Laser Photon Rev 2014;8:458–67.
[47] Sima F, Xu J, Wu D, Sugioka K. Ultrafast laser fabrication of functional biochips: new avenues for exploring 3D micro-and nano-environments. Micromachines 2017;8:40.
[48] Wu D, Niu L-G, Wu S-Z, Xu J, Midorikawa K, Sugioka K. Ship-in-a-bottle femtosecond laser integration of optofluidic microlens arrays with center-pass units enabling coupling-free parallel cell counting with a 100% success rate. Lab Chip 2015;15:1515–23.
[49] Sima F, Serien D, Wu D, et al. In: Micro and nano-biomimetic structures for cell migration study fabricated by hybrid subtractive and additive 3D femtosecond laser processing, Proc. of SPIE, Volume 10092, Laser-based Micro- and Nanoprocessing XI, SPIE LASE, 2017, San Francisco, California, United States, 2017, pp 1009207–1.
[50] Du D, Liu X, Korn G, Squier J, Mourou G. Laser-induced breakdown by impact ionization in SiO_2 with pulse widths from 7 ns to 150 fs. Appl Phys Lett 1994;64:3071–3.
[51] Pronko P, Dutta S, Squier J, Rudd J, Du D, Mourou G. Machining of sub-micron holes using a femtosecond laser at 800 nm. Opt Commun 1995;114:106–10.
[52] Davis KM, Miura K, Sugimoto N, Hirao K. Writing waveguides in glass with a femtosecond laser. Opt Lett 1996;21:1729–31.
[53] Stuart BC, Feit MD, Herman S, Rubenchik A, Shore B, Perry M. Nanosecond-to-femtosecond laser-induced breakdown in dielectrics. Phys Rev B 1996;53:1749.
[54] Miura K, Qiu J, Inouye H, Mitsuyu T, Hirao K. Photowritten optical waveguides in various glasses with ultrashort pulse laser. Appl Phys Lett 1997;71:3329–31.
[55] Sudrie L, Franco M, Prade B, Mysyrowicz A. Writing of permanent birefringent microlayers in bulk fused silica with femtosecond laser pulses. Opt Commun 1999;171:279–84.
[56] Toratani E, Kamata M, Obara M. Self-fabrication of void array in fused silica by femtosecond laser processing. Appl Phys Lett 2005;87:171103.
[57] Juodkazis S, Nishimura K, Tanaka S, et al. Laser-induced microexplosion confined in the bulk of a sapphire crystal: evidence of multimegabar pressures. Phys Rev Lett 2006;96:166101.
[58] Göppert-Mayer M. Über elementarakte mit zwei quantensprüngen. Ann Phys 1931;401:273–94.
[59] LaFratta CN, Fourkas JT, Baldacchini T, Farrer RA. Multiphoton fabrication. Angew Chem Int Ed 2007;46:6238–58.
[60] Fischer J, Mueller JB, Kaschke J, Wolf TJ, Unterreiner A-N, Wegener M. Three-dimensional multi-photon direct laser writing with variable repetition rate. Opt Express 2013;21:26244–60.
[61] Fischer J, Wegener M. Three-dimensional direct laser writing inspired by stimulated-emission-depletion microscopy [invited]. Opt Mater Express 2011;1:614–24.
[62] Choudhury D, Macdonald JR, Kar AK. Ultrafast laser inscription: perspectives on future integrated applications. Laser Photon Rev 2014;8:827–46.
[63] Watanabe W, Asano T, Yamada K, Itoh K, Nishii J. Wavelength division with three-dimensional couplers fabricated by filamentation of femtosecond laser pulses. Opt Lett 2003;28:2491–3.
[64] Liao Y, Xu J, Cheng Y, et al. Electro-optic integration of embedded electrodes and waveguides in linbo 3 using a femtosecond laser. Opt Lett 2008;33:2281–3.
[65] Florea C, Winick KA. Fabrication and characterization of photonicdevices directly written in glass usingfemtosecond laser pulses. J Lightwave Technol 2003;21:246.
[66] Bricchi E, Mills JD, Kazansky PG, Klappauf BG, Baumberg JJ. Birefringent fresnel zone plates in silica fabricated by femtosecond laser machining. Opt Lett 2002;27:2200–2.
[67] Thomson RR, Birks TA, Leon-Saval S, Kar AK, Bland-Hawthorn J. Ultrafast laser inscription of an integrated photonic lantern. Opt Express 2011;19:5698–705.
[68] Osellame R, Chiodo N, Della Valle G, et al. Waveguide lasers in the c-band fabricated by laser inscription with a compact femtosecond oscillator. IEEE J Sel Top Quantum Electron 2006;12:277–85.
[69] del Hoyo J, Moreno-Zárate P, Escalante G, Vallés JA, Fernández P, Solís J. High-efficiency waveguide optical amplifiers and lasers via FS-laser induced local modification of the glass composition. J Lightwave Technol 2017;35:2955–9.
[70] Chen F, Aldana J. Optical waveguides in crystalline dielectric materials produced by femtosecond-laser micromachining. Laser Photonics Rev 2014;8:251–75.
[71] Cerullo G, Osellame R, Taccheo S, et al. Femtosecond micromachining of symmetric waveguides at 1.5 μm by astigmatic beam focusing. Opt Lett 2002;27:1938–40.
[72] Shah L, Arai AY, Eaton SM, Herman PR. Waveguide writing in fused silica with a femtosecond fiber laser at 522 nm and 1 mHz repetition rate. Opt Express 2005;13:1999–2006.
[73] Homoelle D, Wielandy S, Gaeta AL, Borrelli N, Smith C. Infrared photosensitivity in silica glasses exposed to femtosecond laser pulses. Opt Lett 1999;24:1311–3.
[74] Chan JW, Huser TR, Risbud SH, Hayden JS, Krol DM. Waveguide fabrication in phosphate glasses using femtosecond laser pulses. Appl Phys Lett 2003;82:2371–3.
[75] Siegel J, Fernandez-Navarro J, Garcia-Navarro A, et al. Waveguide structures in heavy metal oxide glass written with femtosecond laser pulses above the critical self-focusing threshold. Appl Phys Lett 2005;86:121109.
[76] Efimov O, Glebov L, Richardson K, et al. Waveguide writing in chalcogenide glasses by a train of femtosecond laser pulses. Opt Mater 2001;17:379–86.
[77] Sowa S, Watanabe W, Tamaki T, Nishii J, Itoh K. Symmetric waveguides in poly (methyl methacrylate) fabricated by femtosecond laser pulses. Opt Express 2006;14:291–7.

[78] Thomas J, Heinrich M, Burghoff J, Nolte S, Ancona A, Tünnermann A. Femtosecond laser-written quasi-phase-matched waveguides in lithium niobate. Appl Phys Lett 2007;91:151108.
[79] Beecher S, Thomson R, Reid D, Psaila N, Ebrahim-Zadeh M, Kar A. Strain field manipulation in ultrafast laser inscribed bib 3 o 6 optical waveguides for nonlinear applications. Opt Lett 2011;36:4548–50.
[80] Sotillo B, Bharadwaj V, Hadden J, et al. Diamond photonics platform enabled by femtosecond laser writing. Sci Rep 2016;6:35566.
[81] Torchia G, Rodenas A, Benayas A, Cantelar E, Roso L, Jaque D. Highly efficient laser action in femtosecond-written Nd: yttrium aluminum garnet ceramic waveguides. Appl Phys Lett 2008;92:111103.
[82] Pätzold WM, Demircan A, Morgner U. Low-loss curved waveguides in polymers written with a femtosecond laser. Opt Express 2017;25:263–70.
[83] Lancaster D, Gross S, Ebendorff-Heidepriem H, et al. Fifty percent internal slope efficiency femtosecond direct-written Tm 3+: Zblan waveguide laser. Opt Lett 2011;36:1587–9.
[84] Ajates JG, Romero C, Castillo GR, Chen F, de Aldana JRV. Y-junctions based on circular depressed-cladding waveguides fabricated with femtosecond pulses in Nd:YAG crystal: a route to integrate complex photonic circuits in crystals. Opt Mater 2017;72:220–5.
[85] Castillo GR, Labrador-Páez L, Chen F, Camacho-López S, de Aldana JRV. Depressed-cladding 3-D waveguide arrays fabricated with femtosecond laser pulses. J Lightwave Technol 2017;35:2520–5.
[86] Minzioni P, Osellame R, Sada C, et al. Roadmap for optofluidics. J Opt-Uk 2017;19:093003:1–50.
[87] Gu Y, Bragheri F, Valentino G, Morris K, Bellini N, Osellame R. Ferrofluid-based optofluidic switch using femtosecond laser-micromachined waveguides. Appl Opt 2015;54:1420–5.
[88] Crespi A, Gu Y, Ngamsom B, et al. Three-dimensional Mach-Zehnder interferometer in a microfluidic chip for spatially-resolved label-free detection. Lab Chip 2010;10:1167–73.
[89] Bellini N, Bragheri F, Cristiani I, Guck J, Osellame R, Whyte G. Validation and perspectives of a femtosecond laser fabricated monolithic optical stretcher. Biomed Opt Express 2012;3:2658–68.
[90] Fuqua P, Janson SW, Hansen WW, Helvajian H. In: Fabrication of true 3D microstructures in glass/ceramic materials by pulsed uv laser volumetric exposure techniques. Proceedings of SPIE, Volume 3618, Laser Applications in Microelectronic and Optoelectronic Manufacturing IV; Optoelectronics '99 – Integrated Optoelectronic Devices, San Jose, CA, USA, 1999, pp 213–220.
[91] Masuda M, Sugioka K, Cheng Y, et al. 3-D microstructuring inside photosensitive glass by femtosecond laser excitation. Appl Phys A Mater Sci Process 2003;76:857–60.
[92] Kreibig U. Small silver particles in photosensitive glass: their nucleation and growth. Appl Phys A Mater Sci Process 1976;10:255–64.
[93] Hanada Y, Sugioka K, Kawano H, Ishikawa IS, Miyawaki A, Midorikawa K. Nano-aquarium for dynamic observation of living cells fabricated by femtosecond laser direct writing of photostructurable glass. Biomed Microdevices 2008;10:403–10.
[94] Choudhury D, Ramsay WT, Kiss R, Willoughby NA, Paterson L, Kar AK. A 3D mammalian cell separator biochip. Lab Chip 2012;12:948–53.
[95] Paiè P, Bragheri F, Vazquez RM, Osellame R. Straightforward 3D hydrodynamic focusing in femtosecond laser fabricated microfluidic channels. Lab Chip 2014;14:1826–33.
[96] Chen F, Shan C, Liu K, et al. Process for the fabrication of complex three-dimensional microcoils in fused silica. Opt Lett 2013;38:2911–4.
[97] Choudhury D, Rodenas A, Paterson L, Díaz F, Jaque D, Kar AK. Three-dimensional microstructuring of yttrium aluminum garnet crystals for laser active optofluidic applications. Appl Phys Lett 2013;103:041101.
[98] Hanada Y, Ogawa T, Koike K, Sugioka K. Making the invisible visible: a microfluidic chip using a low refractive index polymer. Lab Chip 2016;16:2481–6.
[99] Tokel O, Turnalı A, Makey G, et al. In-chip microstructures and photonic devices fabricated by nonlinear laser lithography deep inside silicon. Nat Photonics 2017;11:639–45.
[100] Kerse C, Kalaycıoğlu H, Elahi P, et al. Ablation-cooled material removal with ultrafast bursts of pulses. Nature 2016;537:84–8.
[101] Li Y, Itoh K, Watanabe W, et al. Three-dimensional hole drilling of silica glass from the rear surface with femtosecond laser pulses. Opt Lett 2001;26:1912–4.
[102] Hwang D, Choi T, Grigoropoulos C. Liquid-assisted femtosecond laser drilling of straight and three-dimensional microchannels in glass. Appl Phys A Mater Sci Process 2004;79:605–12.
[103] Ke K, Hasselbrink EF, Hunt AJ. Rapidly prototyped three-dimensional nanofluidic channel networks in glass substrates. Anal Chem 2005;77:5083–8.
[104] Vaezi M, Seitz H, Yang SF. A review on 3D micro-additive manufacturing technologies. Int J Adv Manuf Technol 2013;67:1721–54.
[105] Malinauskas M, Zukauskas A, Hasegawa S, et al. Ultrafast laser processing of materials: from science to industry. Light Sci Appl 2016;5:e16133.
[106] Sugioka K, Cheng Y. Femtosecond laser three-dimensional micro- and nanofabrication. Appl Phys Rev 2014;1:041303: 1–35.
[107] Maruo S, Saeki T. Femtosecond laser direct writing of metallic microstructures by photoreduction of silver nitrate in a polymer matrix. Opt Express 2008;16:1174–9.
[108] Nie B, Yang LM, Huang H, Bai S, Wan P, Liu J. Femtosecond laser additive manufacturing of iron and tungsten parts. Appl Phys A Mater 2015;119:1075–80.
[109] Xu J, Kawano H, Liu W, et al. Controllable alignment of elongated microorganisms in 3D microspace using electrofluidic devices manufactured by hybrid femtosecond laser microfabrication. Microsyst Nanoeng 2017;3:16078.
[110] Xu J, Wu D, Hanada Y, et al. Electrofluidics fabricated by space-selective metallization in glass microfluidic structures using femtosecond laser direct writing. Lab Chip 2013;13:4608–16.
[111] Shukla S, Vidal X, Furlani EP, et al. Subwavelength direct laser patterning of conductive gold nanostructures by simultaneous photopolymerization and photoreduction. ACS Nano 2011;5:1947–57.
[112] Xiong W, Liu Y, Jiang LJ, et al. Laser-directed assembly of aligned carbon nanotubes in three dimensions for multifunctional device fabrication. Adv Mater 2016;28:2002–9.
[113] Sun HB, Kawata S. Two-photon photopolymerization and 3D lithographic microfabrication. Adv Polym Sci 2004;170:169–273.

[114] Connell JL, Wessel AK, Parsek MR, Ellington AD, Whiteley M, Shear JB. Probing prokaryotic social behaviors with bacterial "lobster traps". mBio 2010;1:e00202–10.
[115] Deubel M, Von Freymann G, Wegener M, Pereira S, Busch K, Soukoulis CM. Direct laser writing of three-dimensional photonic-crystal templates for telecommunications. Nat Mater 2004;3:444–7.
[116] Formanek F, Takeyasu N, Tanaka T, Chiyoda K, Ishikawa A, Kawata S. Three-dimensional fabrication of metallic nanostructures over large areas by two-photon polymerization. Opt Express 2006;14:800–9.
[117] Kelemen L, Valkai S, Ormos P. Parallel photopolymerisation with complex light patterns generated by diffractive optical elements. Opt Express 2007;15:14488–97.
[118] Vizsnyiczai G, Kelemen L, Ormos P. Holographic multi-focus 3D two-photon polymerization with real-time calculated holograms. Opt Express 2014;22:24217–23.
[119] Kondo T, Juodkazis S, Mizeikis V, Matsuo S, Misawa H. Fabrication of three-dimensional periodic microstructures in photoresist SU-8 by phase-controlled holographic lithography. New J Phys 2006;8:250.
[120] Ricci D, Nava MM, Zandrini T, Cerullo G, Raimondi MT, Osellame R. Scaling-up techniques for the nanofabrication of cell culture substrates via two-photon polymerization for industrial-scale expansion of stem cells. Materials 2017;10:66.
[121] Jiang L, Campbell J, Lu Y, Bernat T, Petta N. Direct writing target structures by two-photon polymerization. Fusion Sci Technol 2016;70:295–309.
[122] Poocza L, Gottschaldt M, Markweg E, et al. Optimized photoinitiator for fast two-photon absorption polymerization of polyester-macromers for tissue engineering. Adv Eng Mater 2017;19:1600686.
[123] Li LJ, Gattass RR, Gershgoren E, Hwang H, Fourkas JT. Achieving lambda/20 resolution by one-color initiation and deactivation of polymerization. Science 2009;324:910–3.
[124] Gan Z, Cao Y, Evans RA, Gu M. Three-dimensional deep subdiffraction optical beam lithography with 9 nm feature size. Nat Commun 2013;4:2061.
[125] Serbin J, Ovsianikov A, Chichkov B. Fabrication of woodpile structures by two-photon polymerization and investigation of their optical properties. Opt Express 2004;12:5221–8.
[126] Haque M, Zacharia NS, Ho S, Herman PR. Laser-written photonic crystal optofluidics for electrochromatography and spectroscopy on a chip. Biomed Opt Express 2013;4:1472–85.
[127] Guo R, Xiao SZ, Zhai XM, Li JW, Xia AD, Huang WH. Micro lens fabrication by means of femtosecond two photon photopolymerization. Opt Express 2006;14:810–6.
[128] Xu JJ, Yao WG, Tian ZN, et al. High curvature concave-convex microlens. IEEE Photonics Technol Lett 2015;27:2465–8.
[129] Cojoc G, Liberale C, Candeloro P, et al. Optical micro-structures fabricated on top of optical fibers by means of two-photon photopolymerization. Microelectron Eng 2010;87:876–9.
[130] Zukauskas A, Melissinaki V, Kaskelyte D, Farsari M, Malinauskas M. Improvement of the fabrication accuracy of fiber tip microoptical components via mode field expansion. J Laser Micro Nanoeng 2014;9:68–72.
[131] Li Y, Yu YS, Guo L, et al. High efficiency multilevel phase-type fresnel zone plates produced by two-photon polymerization of SU-8. J Opt-Uk 2010;12:035203.
[132] Wu D, Xu J, Niu L-G, Wu S-Z, Midorikawa K, Sugioka K. In-channel integration of designable microoptical devices using flat scaffold-supported femtosecond-laser microfabrication for coupling-free optofluidic cell counting. Light Sci Appl 2015;4:e228.
[133] Wang J, He Y, Xia H, et al. Embellishment of microfluidic devices via femtosecond laser micronanofabrication for chip functionalization. Lab Chip 2010;10:1993–6.
[134] Xu B, Du WQ, Li JW, et al. High efficiency integration of three-dimensional functional microdevices inside a microfluidic chip by using femtosecond laser multifoci parallel microfabrication. Sci Rep 2016;6:19989–9.
[135] Xu B, Hu WJ, Du WQ, et al. Arch-like microsorters with multimodal and clogging-improved filtering functions by using femtosecond laser multifocal parallel microfabrication. Opt Express 2017;25:16739–53.
[136] Lim TW, Son Y, Jeong YJ, et al. Three-dimensionally crossing manifold micro-mixer for fast mixing in a short channel length. Lab Chip 2011;11:100–3.
[137] Maruo S, Takaura A, Saito Y. Optically driven micropump with a twin spiral microrotor. Opt Express 2009;17:18525–32.
[138] Kelemen L, Valkai S, Ormos P. Integrated optical motor. Appl Opt 2006;45:2777–80.
[139] Villangca MJ, Palima D, Banas AR, Gluckstad J. Light-driven micro-tool equipped with a syringe function. Light Sci Appl 2016;5:e16148.
[140] Liu YJ, Yang JY, Nie YM, et al. A simple and direct reading flow meter fabricated by two-photon polymerization for microfluidic channel. Microfluid Nanofluidics 2015;18:427–31.
[141] Phillips DB, Simpson SH, Grieve JA, et al. Force sensing with a shaped dielectric micro-tool. EPL Europhys Lett 2012;99:58004.
[142] Palima D, Banas AR, Vizsnyiczai G, Kelemen L, Ormos P, Gluckstad J. Wave-guided optical waveguides. Opt Express 2012;20:2004–14.
[143] Vizsnyiczai G, Lestyan T, Joniova J, et al. Optically trapped surface-enhanced raman probes prepared by silver photoreduction to 3D microstructures. Langmuir 2015;31:10087–93.
[144] Vizsnyiczai G, Aekbote BL, Buzas A, Grexa I, Ormos P, Kelemen L. High accuracy indirect optical manipulation of live cells with functionalized microtools. In: Dholakia K, Spalding GC, eds. Optical trapping and optical micromanipulation XIII, San Diego, CA, USA, SPIE, 2016, Vol. 9922, 92216.
[145] Asavei T, Nieminen TA, Loke VLY, et al. Optically trapped and driven paddle-wheel. New J Phys 2013;15:17.
[146] Aekbote BL, Fekete T, Jacak J, Vizsnyiczai G, Ormos P, Kelemen L. Surface-modified complex SU-8 microstructures for indirect optical manipulation of single cells. Biomed Opt Express 2016;7:45–56.
[147] Melissinaki V, Gill AA, Ortega I, et al. Direct laser writing of 3D scaffolds for neural tissue engineering applications. Biofabrication 2011;3:045005.
[148] Weiss T, Hildebrand G, Schade R, Liefeith K. Two-photon polymerization for microfabrication of three-dimensional scaffolds for tissue engineering application. Eng Life Sci 2009;9:384–90.
[149] Klein F, Richter B, Striebel T, et al. Two-component polymer scaffolds for controlled three-dimensional cell culture. Adv Mater 2011;23:1341–5.
[150] Torgersen J, Qin XH, Li ZQ, Ovsianikov A, Liska R, Stampfl J. Hydrogels for two-photon polymerization: a toolbox for mimicking the extracellular matrix. Adv Funct Mater 2013;23:4542–54.

[151] Kufelt O, El-Tamer A, Sehring C, Meissner M, Schlie-Wolter S, Chichkov BN. Water-soluble photopolymerizable chitosan hydrogels for biofabrication via two-photon polymerization. Acta Biomater 2015;18:186–95.
[152] Kim M, Hwang DJ, Jeon H, Hiromatsu K, Grigoropoulos CP. Single cell detection using a glass-based optofluidic device fabricated by femtosecond laser pulses. Lab Chip 2009;9:311–8.
[153] Bragheri F, Minzioni P, Vazquez RM, et al. Optofluidic integrated cell sorter fabricated by femtosecond lasers. Lab Chip 2012;12:3779–84.
[154] Maselli V, Grenier JR, Ho S, Herman PR. Femtosecond laser written optofluidic sensor: Bragg grating waveguide evanescent probing of microfluidic channel. Opt Express 2009;17:11719–29.
[155] Xu J, Wu D, Hanada Y, et al. Electrofluidics fabricated by space-selective metallization in glass microfluidic structures using femtosecond laser direct writing. Lab Chip 2013;13:4608–16.
[156] Jonušauskas L, Rekštyte S, Buividas R, et al. Hybrid subtractive-additive-welding microfabrication for lab-on-chip applications via single amplified femtosecond laser source. Opt Eng 2017;56:094108.
[157] Wu D, Xu J, Niu L-G, Wu S-Z, Midorikawa K, Sugioka K. In-channel integration of designable microoptical devices using flat scaffold-supported femtosecond-laser microfabrication for coupling-free optofluidic cell counting. Light Sci Appl 2015;4:e228.
[158] Sima F, Wu D, Xu J, Midorikawa K, Sugioka K. In: Roth S, Nakata Y, Neuenschwander B, Xu X, eds. Ship-in-a-bottle integration by hybrid femtosecond laser technology for fabrication of true 3D biochips, Proc. SPIE 9350, Laser Applications in Microelectronic and Optoelectronic Manufacturing (LAMOM) XX, San Francisco, California, USA, SPIE LASE; International Society for Optics and Photonics, 2015, 93500F-93500F-93508.